800 MeV Proton Radiography

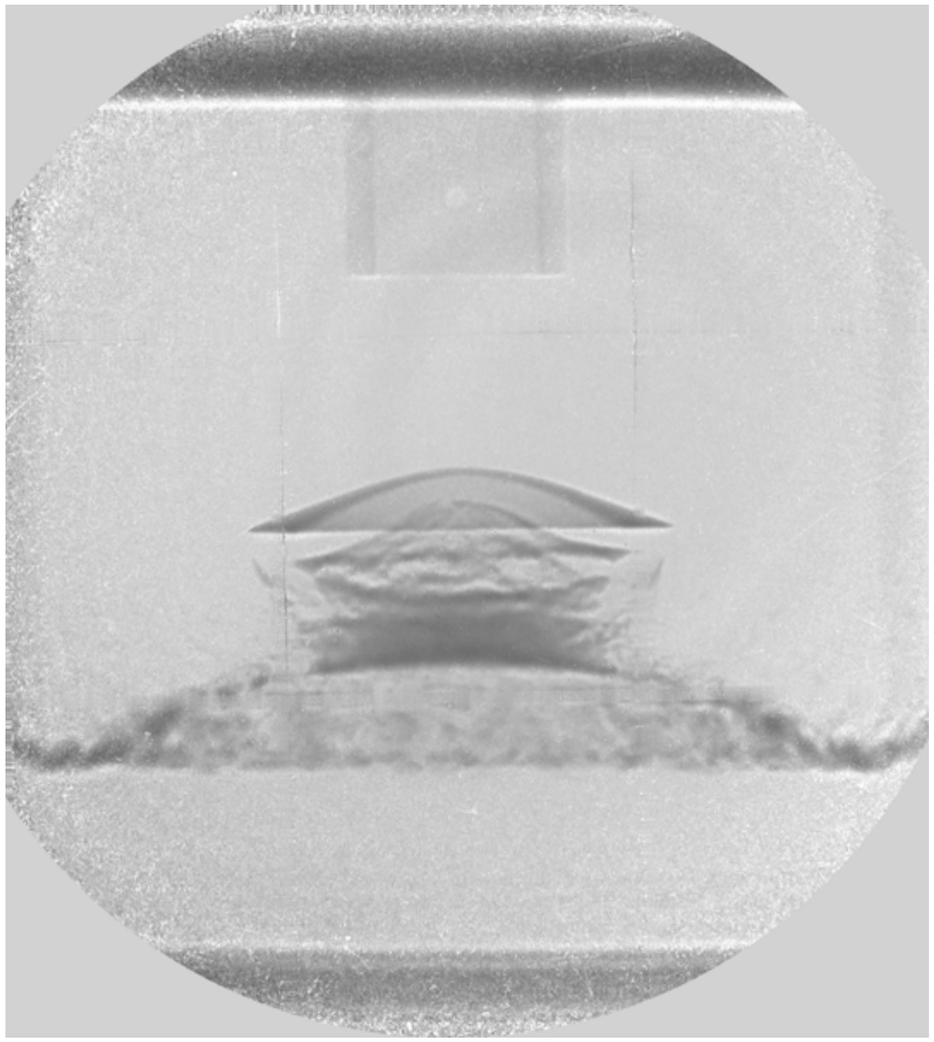

Frank Merrill, LANL
and the pRad collaboration

pRad Team

NSTec

Alfred Meidinger, Josh Tybo, Doug Lewis

DE-3

Joe Bainbridge, Robert Lopez, Mark Marr-Lyon, Paul Rightley

HX-4

Wendy McNeil

LANSCE-NS

Leo Bittecker

P-23

Nick King, Kris Kwiatkowski, Paul Nedrow, Gary Grim

P-25

Deborah Clark, Camilo Espinoza, Gary Hogan, Brian Hollander, Julian Lopez, Fesseha Mariam, Frank Merrill, Christopher Morris, Matthew Murray, Alexander Saunders, Cynthia Schwartz, Terry N. Thompson, Dale Tupa, Eduardo Campos

S-7

Rodger Liljestrand

LANSCE Experimental Areas

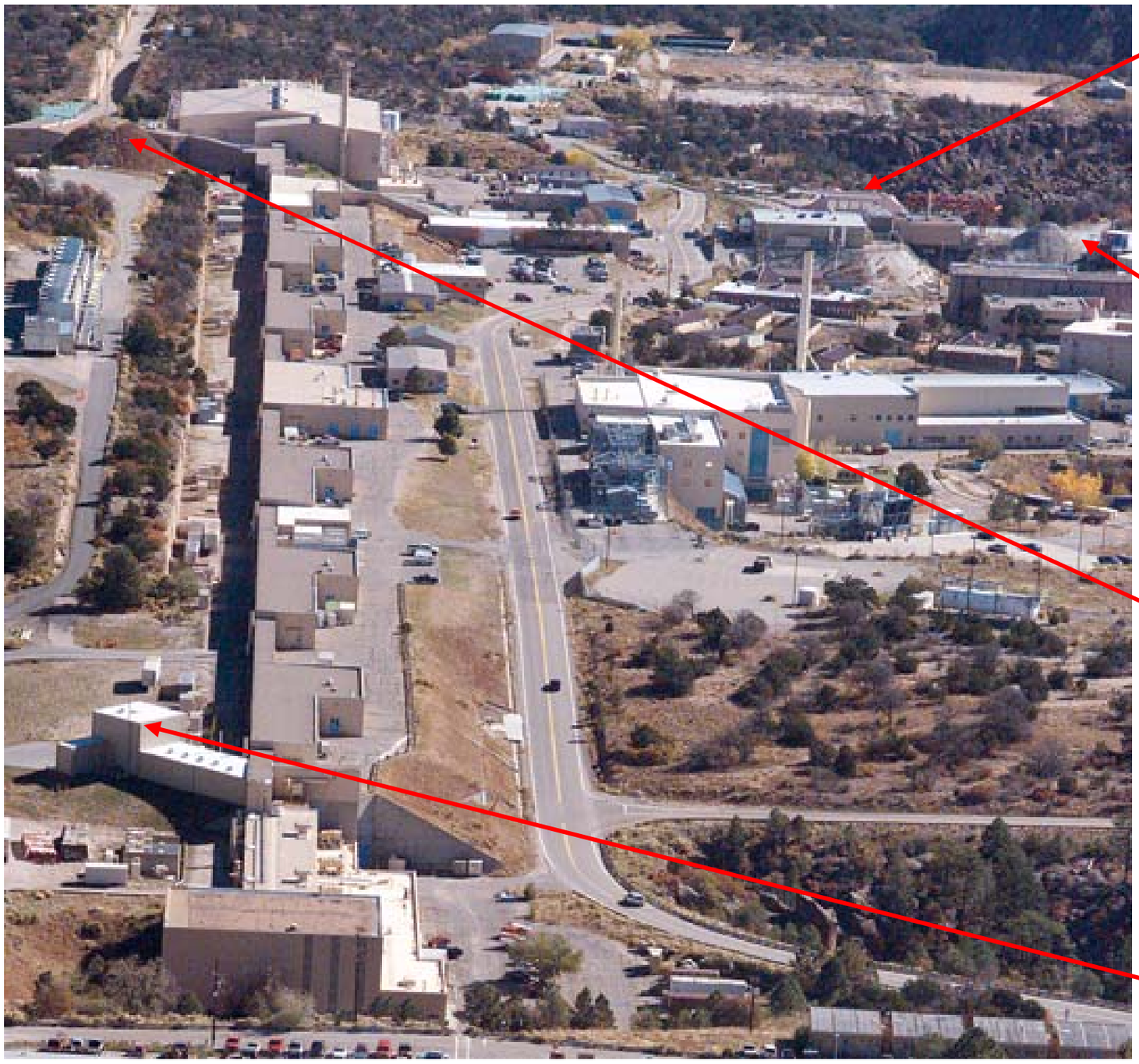

- Lujan Center
  - ***National security research***
  - ***Materials, bio-science, and nuclear physics***
  - ***National user facility***
- WNR
  - ***National security research***
  - ***Nuclear Physics***
  - ***Neutron Irradiation***
- Proton Radiography
  - ***National security research***
  - ***Dynamic Materials science,***
  - ***Hydrodynamics***
- Isotope Production Facility
  - ***Medical radioisotopes***

800 MeV pRad Facility at LANSCE

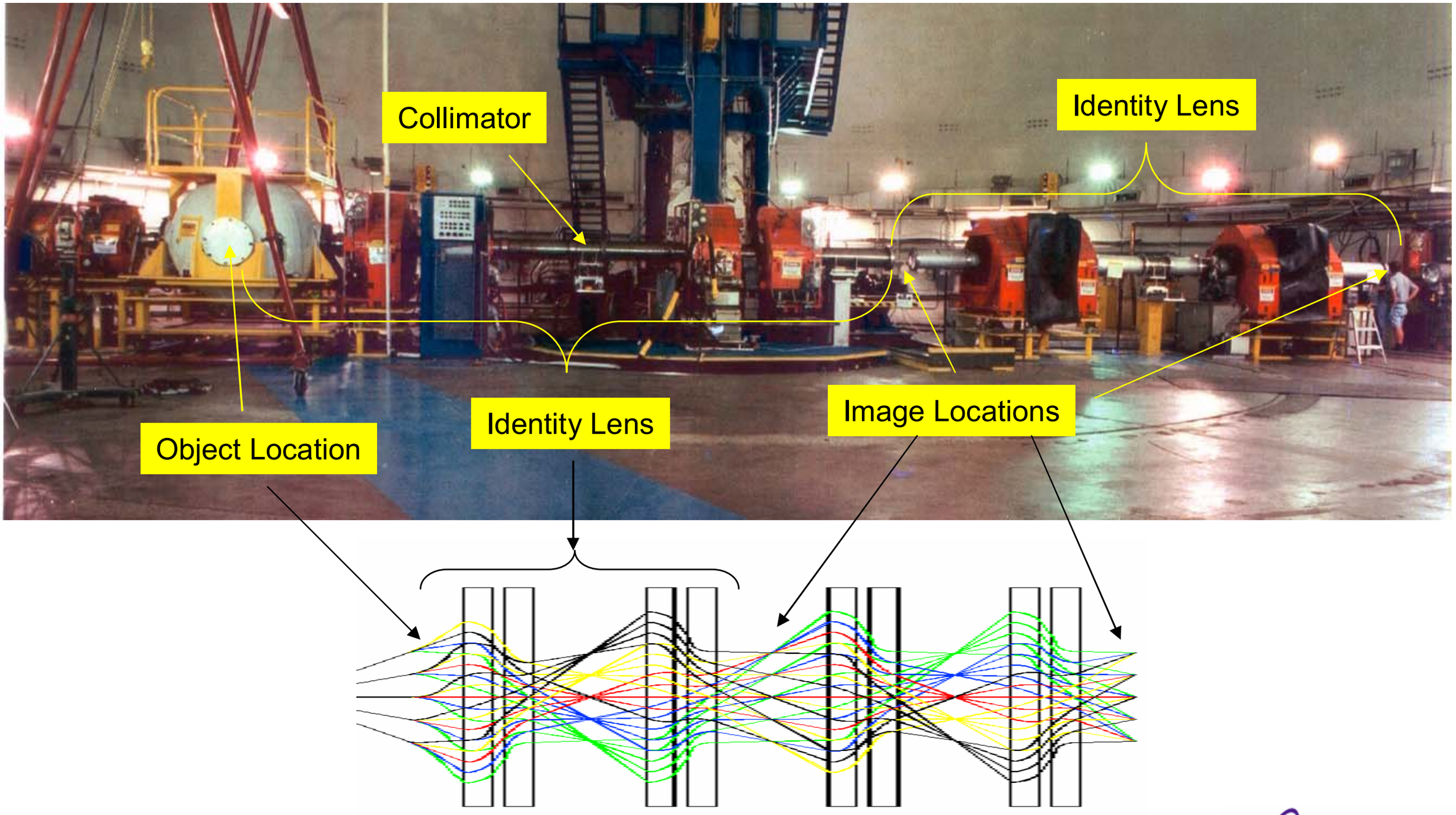

Temporal Resolution

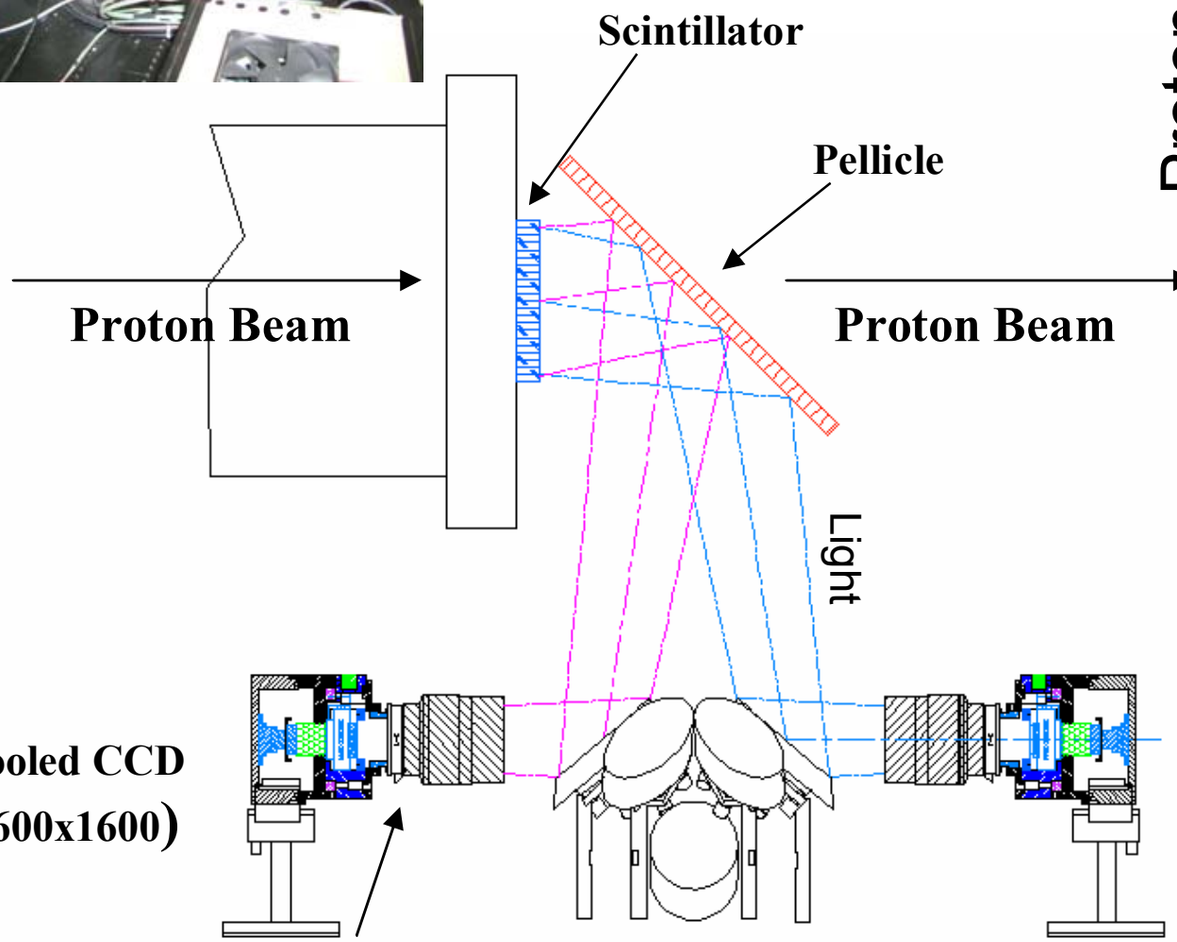

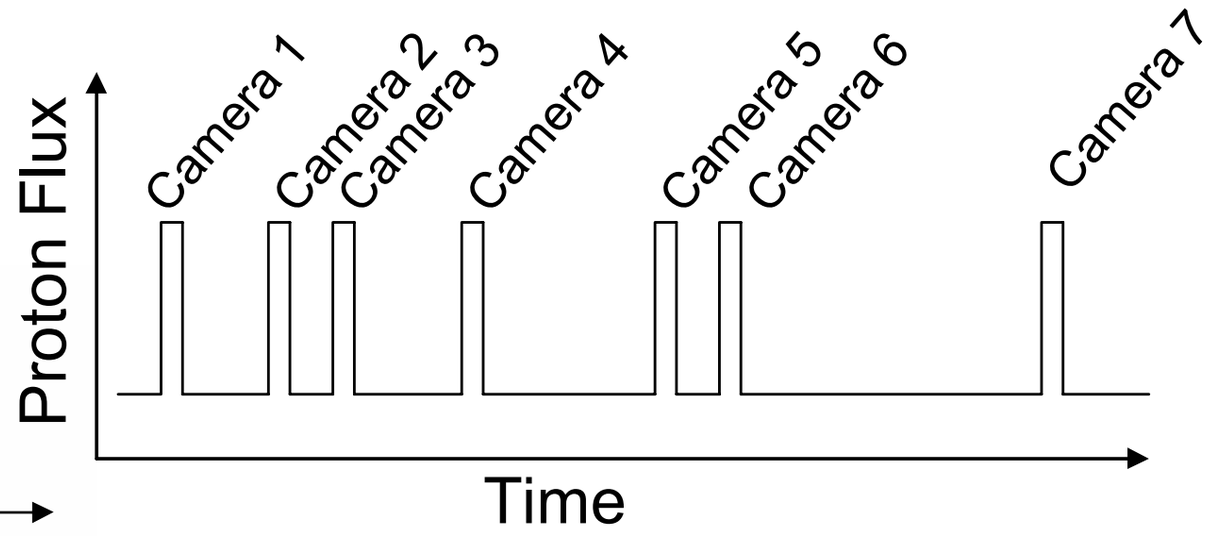

- 19 images at first station
- 22 images at second station
- Typically 100 ns exposure times
- 180 ns inter frame spacing
- Beam available for1000 μs at 1 Hz

Resolution of 12” Lens

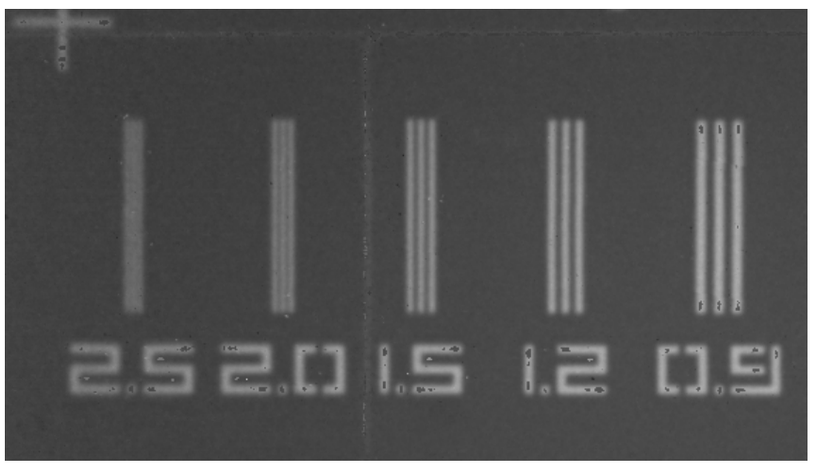

- Bare resolution (rms)
  - Station 1: 178 μm
  - Station 2: 280 μm

Gaussian Line Spread Function

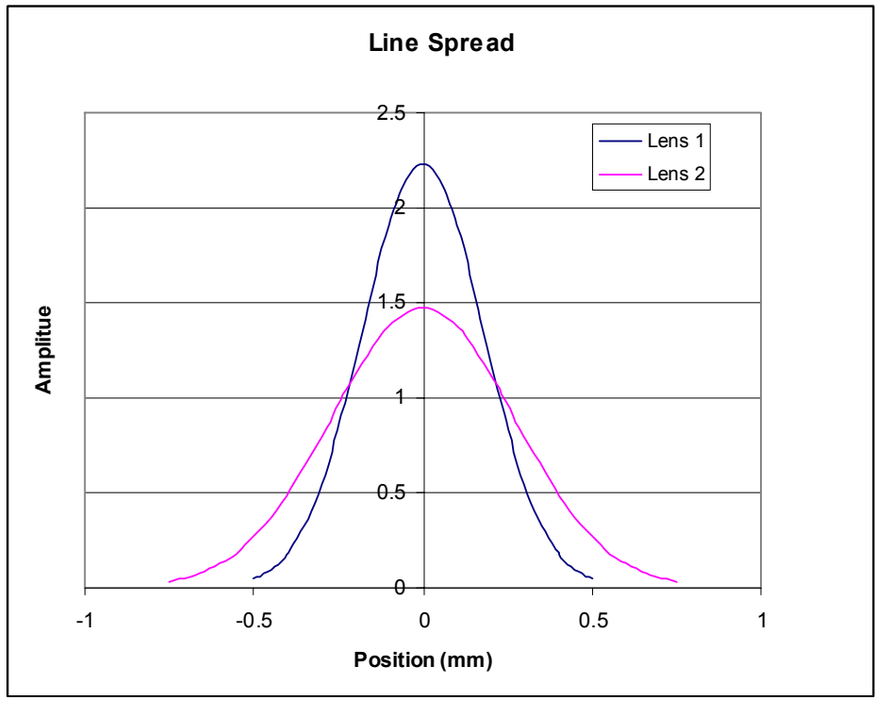

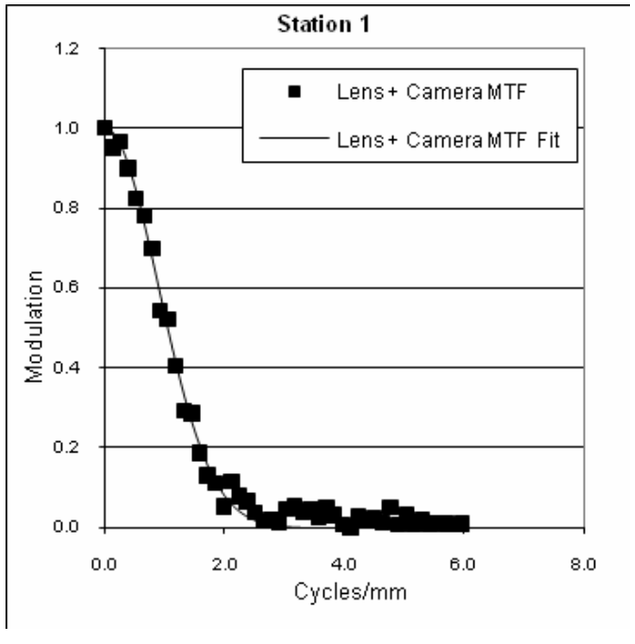

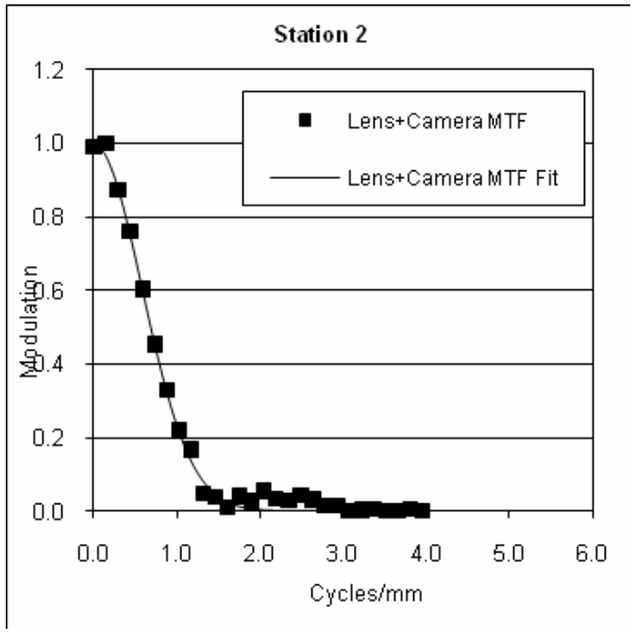

X3 Magnifier

X3 Magnifier

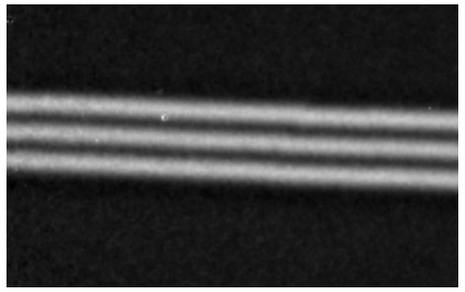

2.5 lp/mm

- 4 inch lens
- Station 1: 65 μm
- Gaussian blur function.
- 42 mm field of view

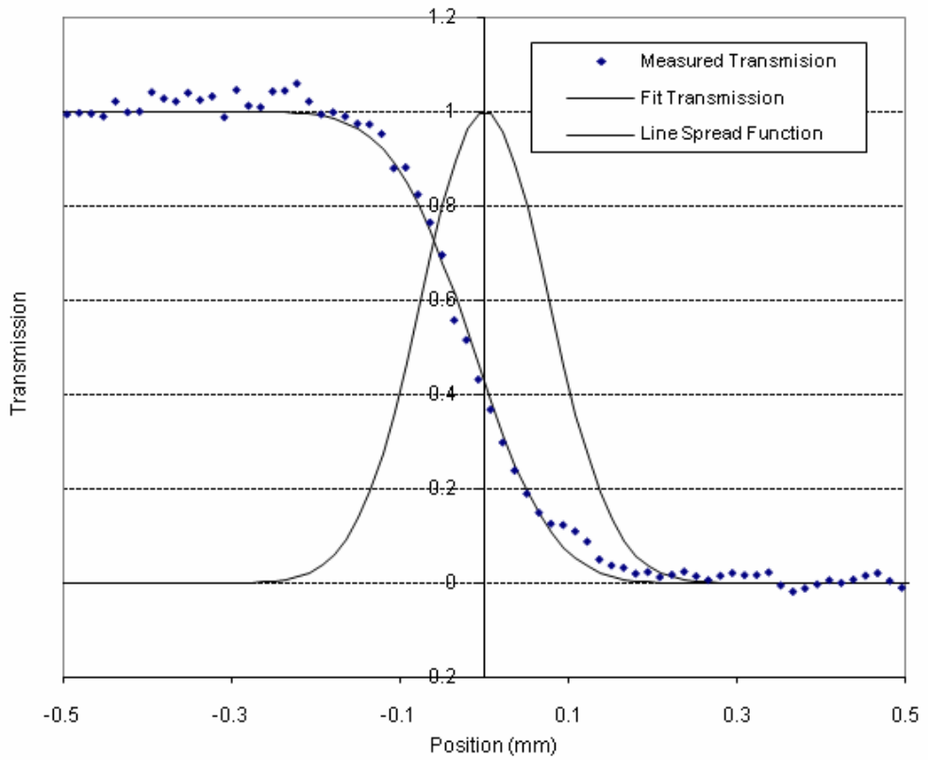

X7 Magnifier

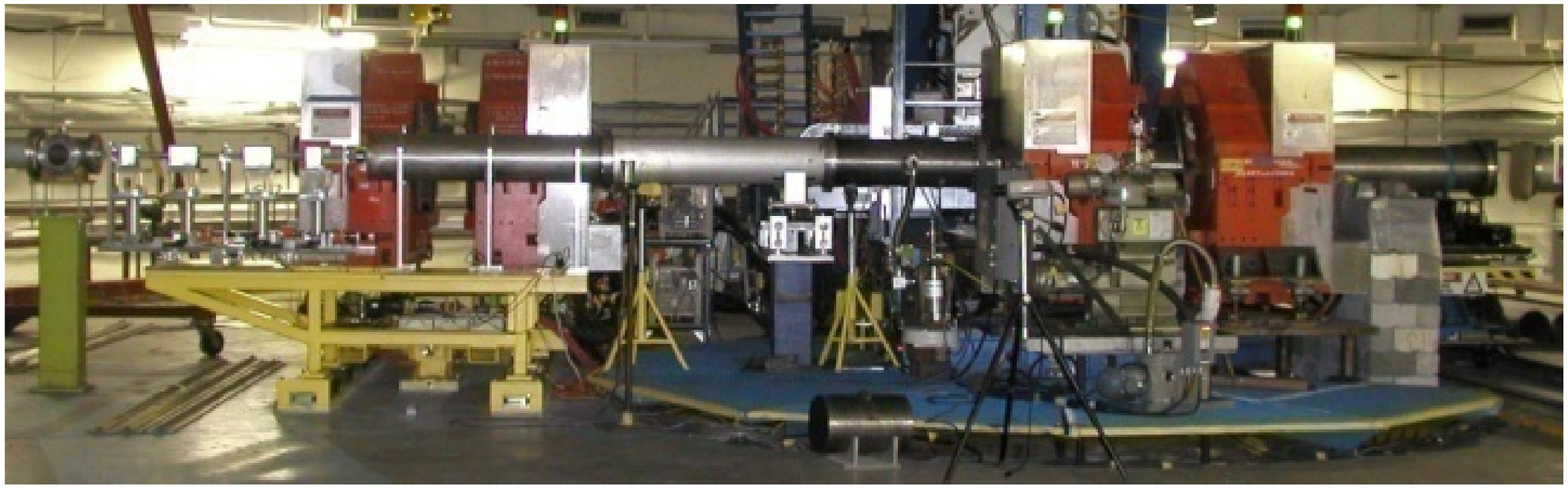

- 1 inch lens
- Station 1: 30 μm
- Gaussian blur function.
- 17 mm field of view

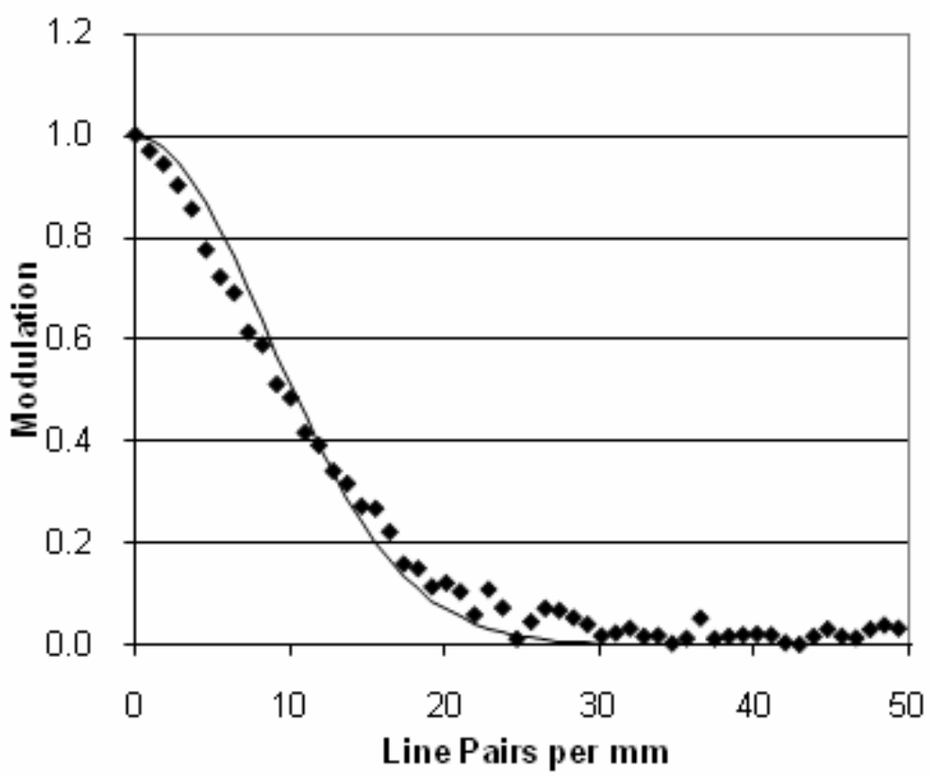

Powder Gun Driven Equation Of State Measurements

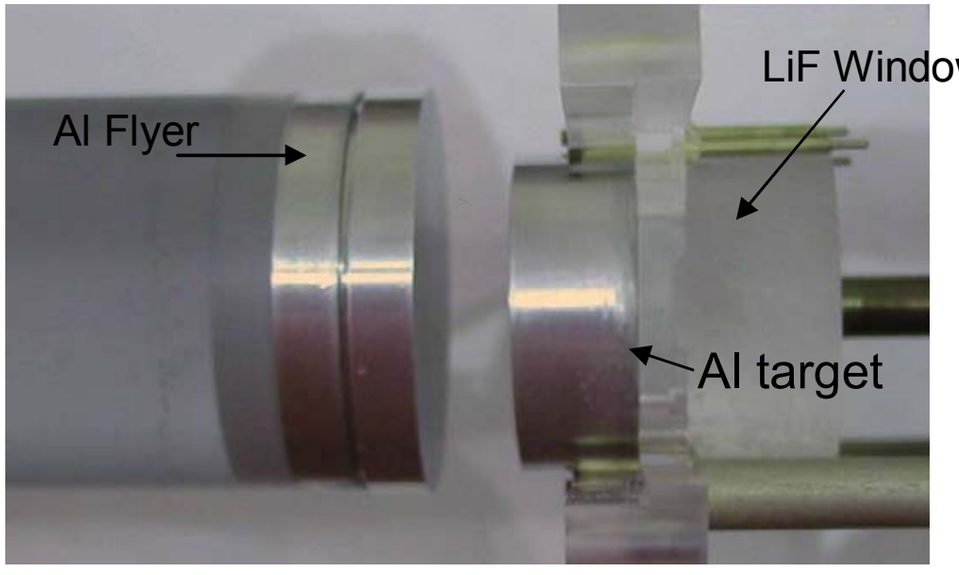

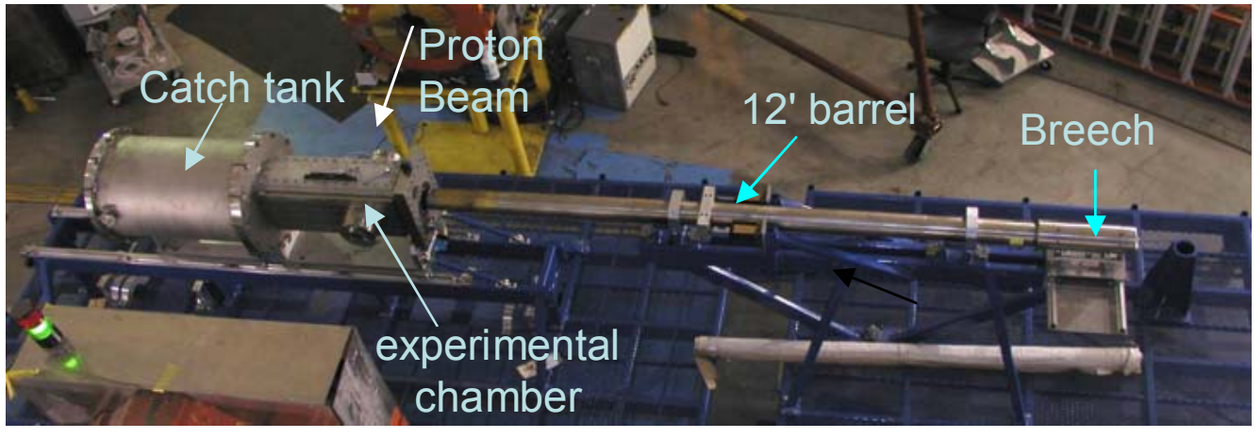

Aluminum

1.4 km/s

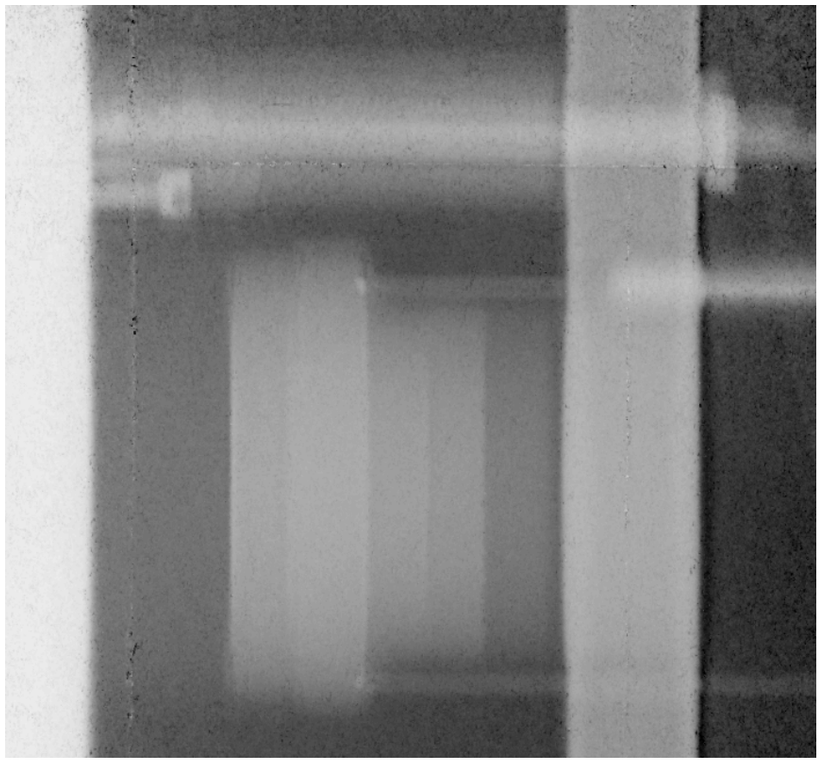

Copper

1.4 km/s

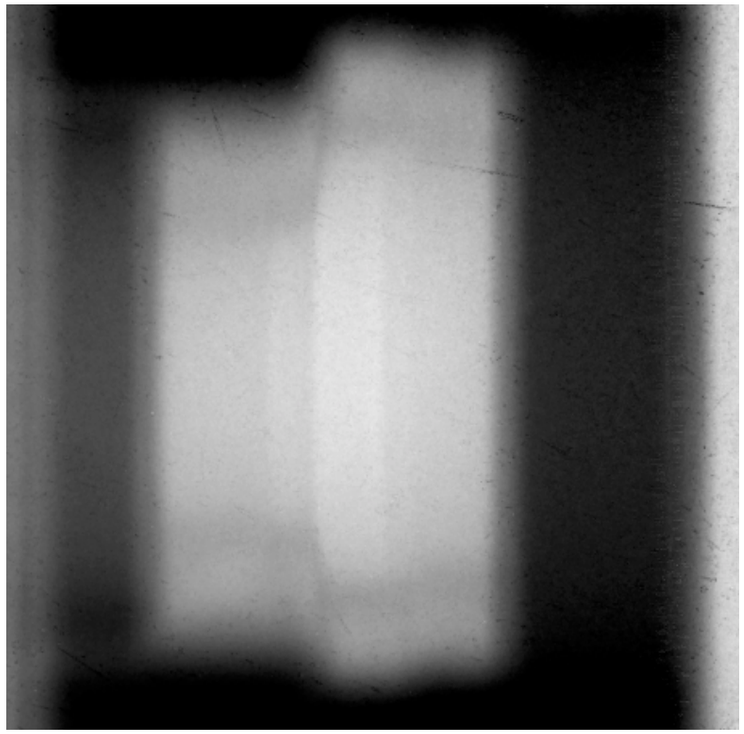

Powder Gun Al/Cu Equation Of State

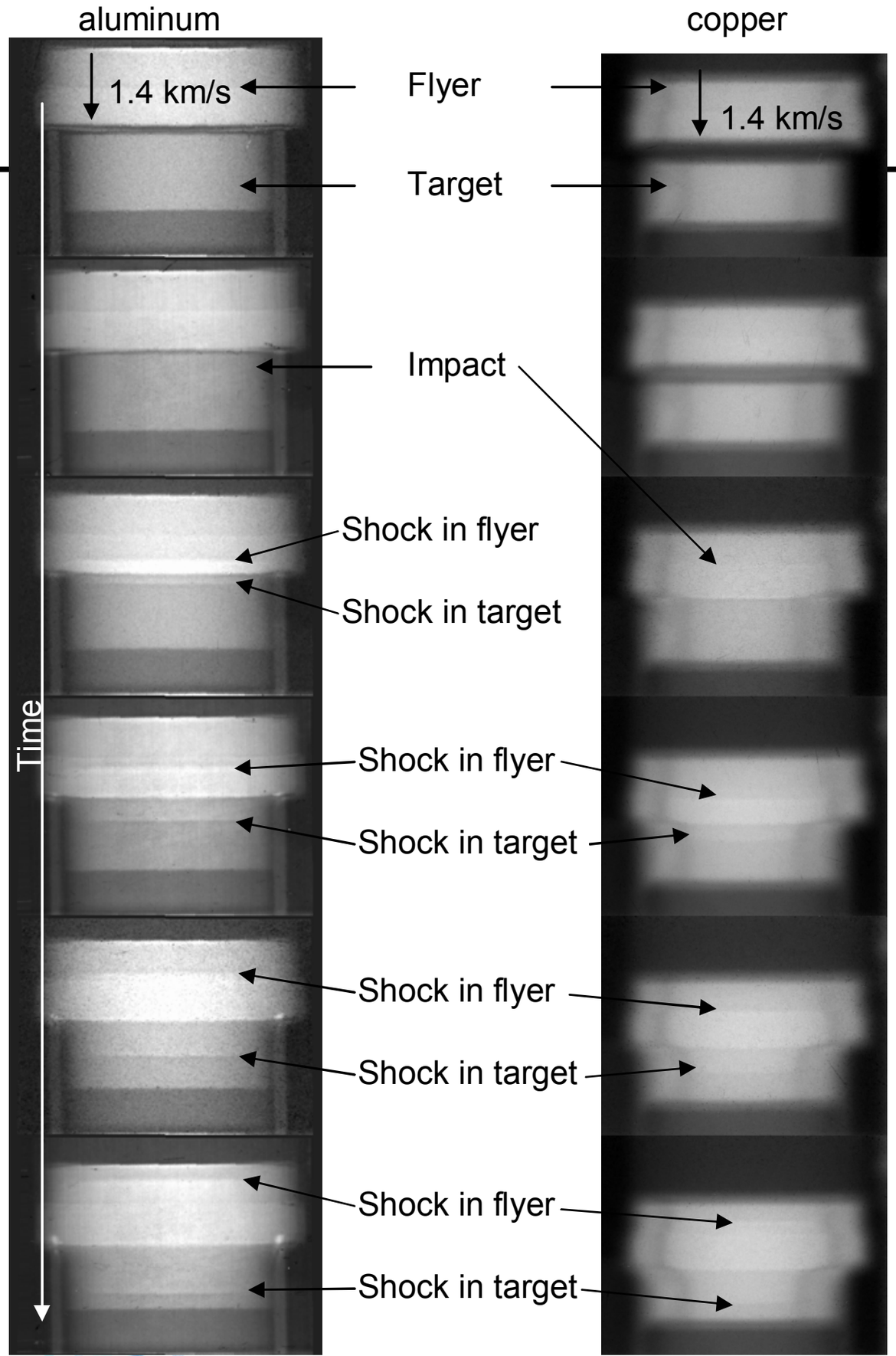

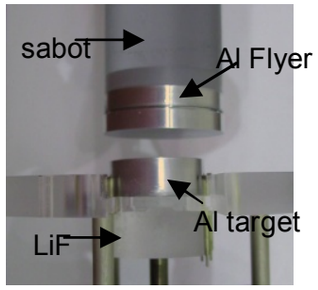

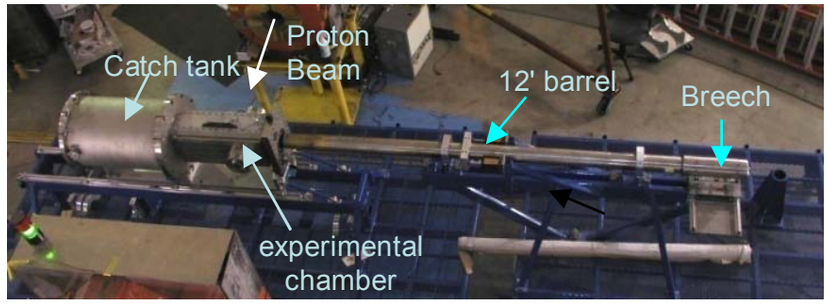

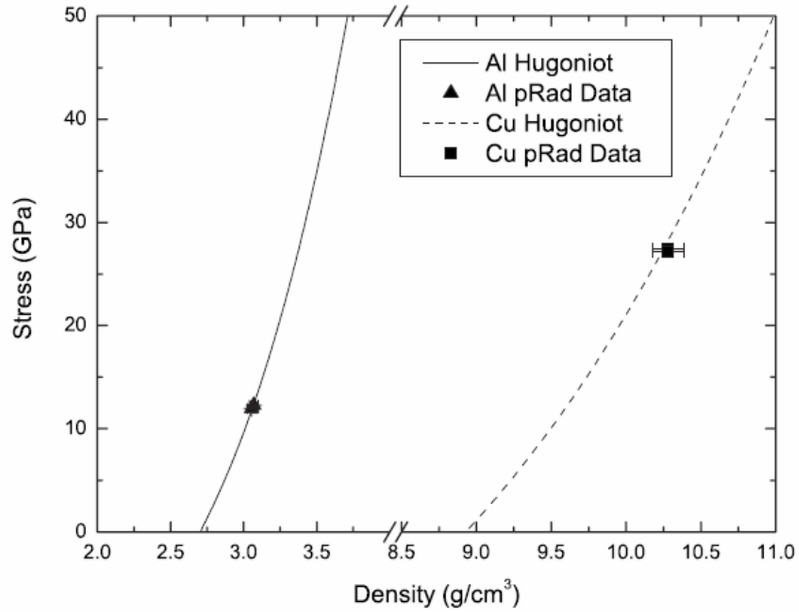

TABLE I. Summary of the experiments with the uncertainties for each quantity shown in parentheses.

Experiment	Impactor/ sample	Impactor velocity (mm/μs)	Peak stress (GPa)	Initial density (g/cm^3)	Calculated density (g/cm^3)	Measured density (g/cm^3)	Agreement
1	Al 6061-T6	1.452 (0.012)	12.27 (0.11)	2.710 (0.003)	3.067 (0.005)	3.070 (0.025)	0.1%
2	Al 6061-T6	1.422 (0.002)	11.98 (0.03)	2.710 (0.003)	3.060 (0.004)	3.056 (0.020)	0.1%
3	OFHC Cu	1.30 (0.04)	28.59 (0.91)	8.928 (0.003)	10.30 (0.05)	10.28 (0.08)	0.2%
4	OFHC Cu	1.249 (0.002)	27.16 (0.06)	8.928 (0.003)	10.241 (0.006)	10.28 (0.08)	0.4%

Solid-Solid Phase Transitions in Iron

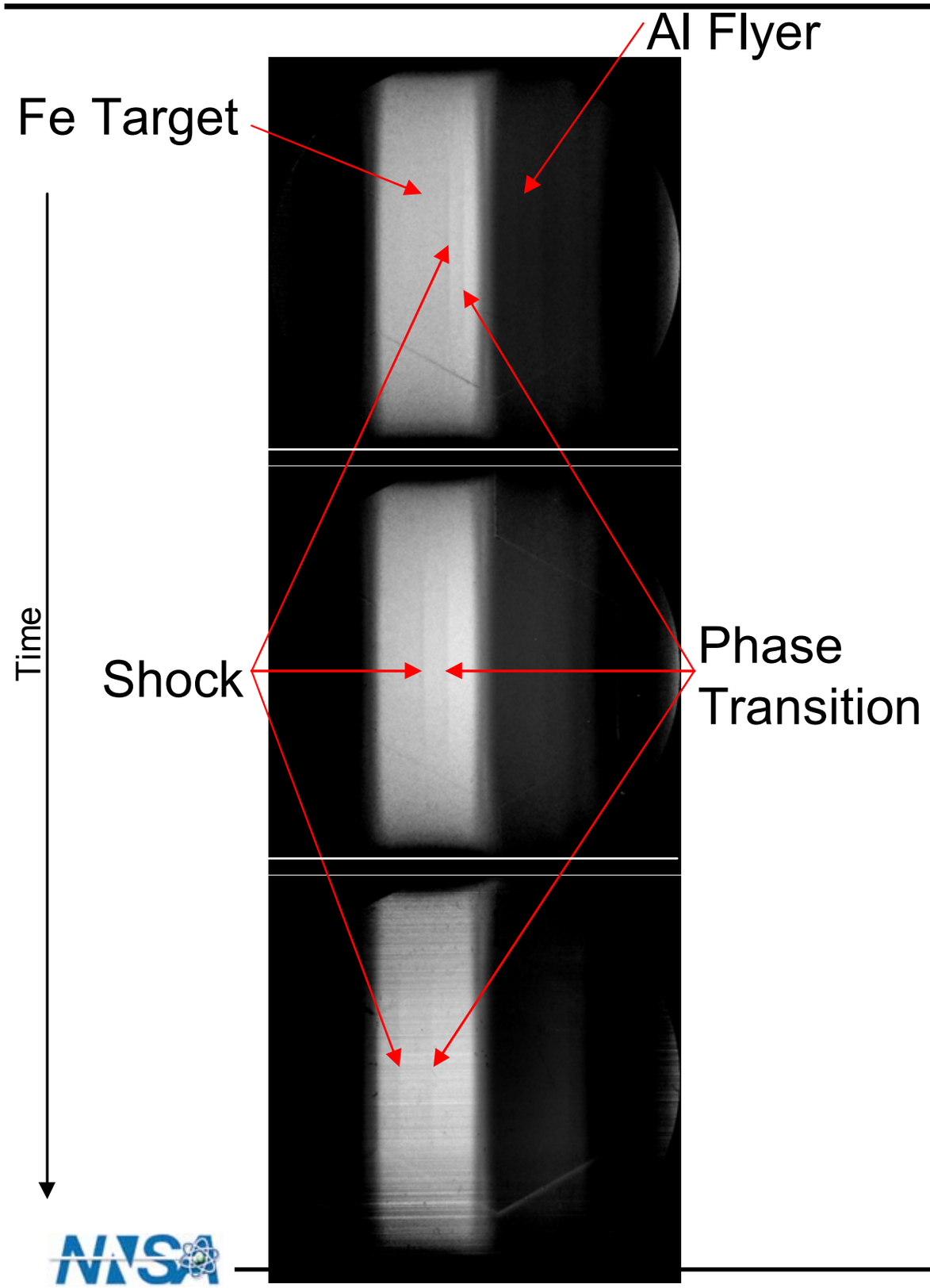

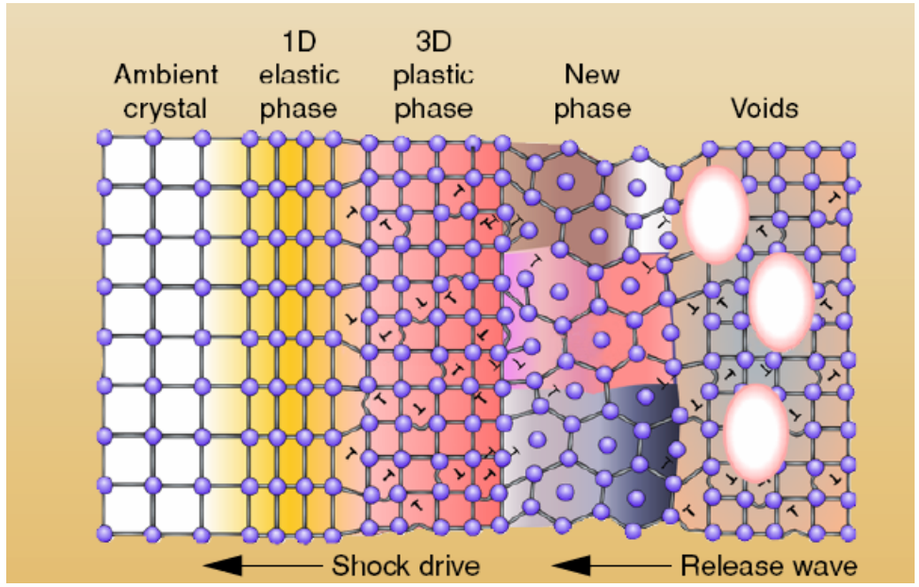

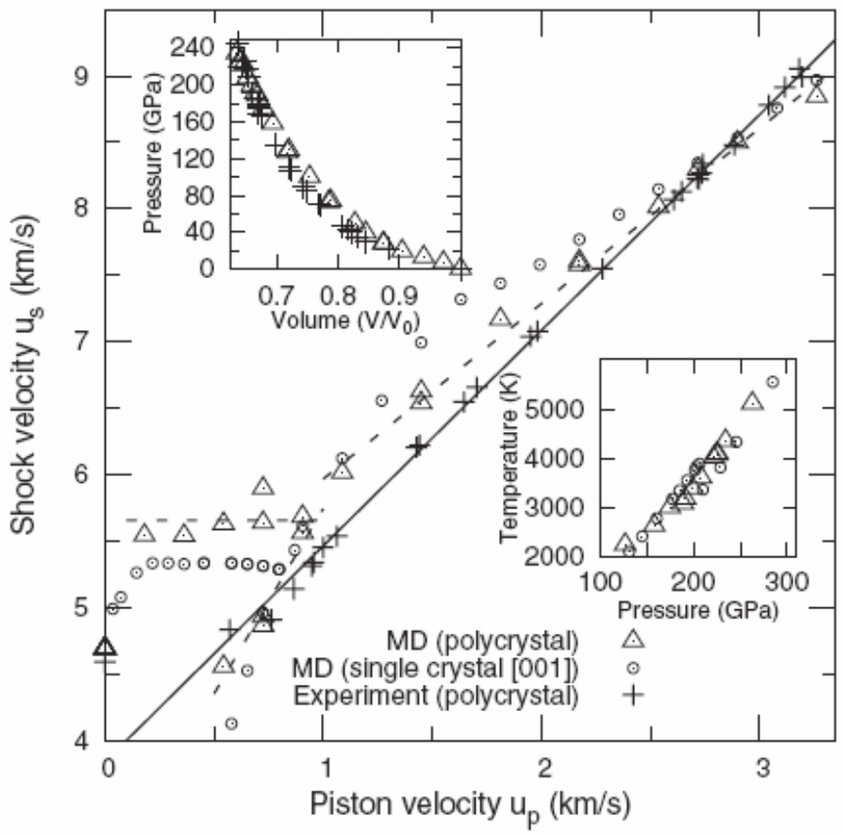

Phys. Rev. Lett. 98 135701 (2007)

pRad has been used to study the failure of materials driven by point detonated high explosives

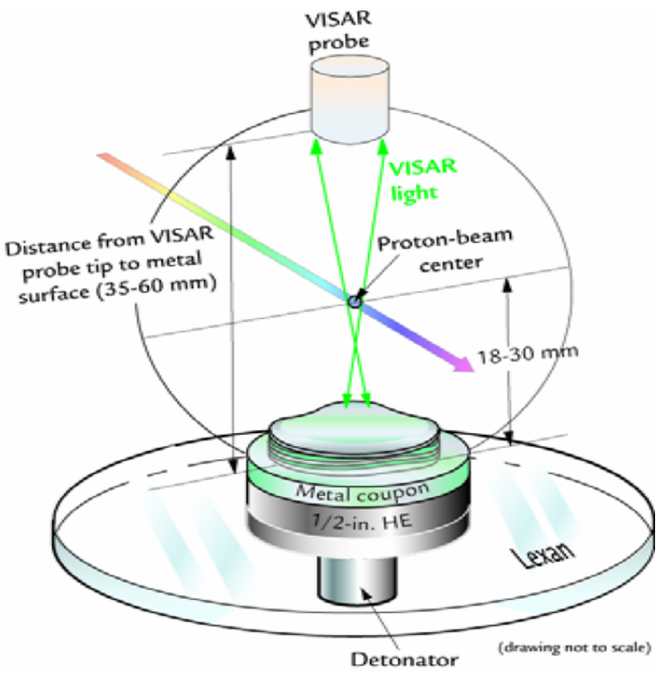

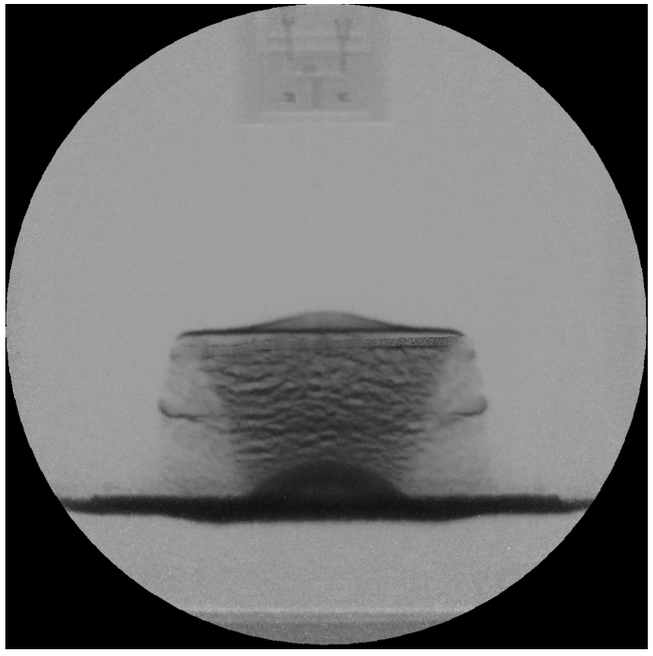

A comparison of spall for different materials

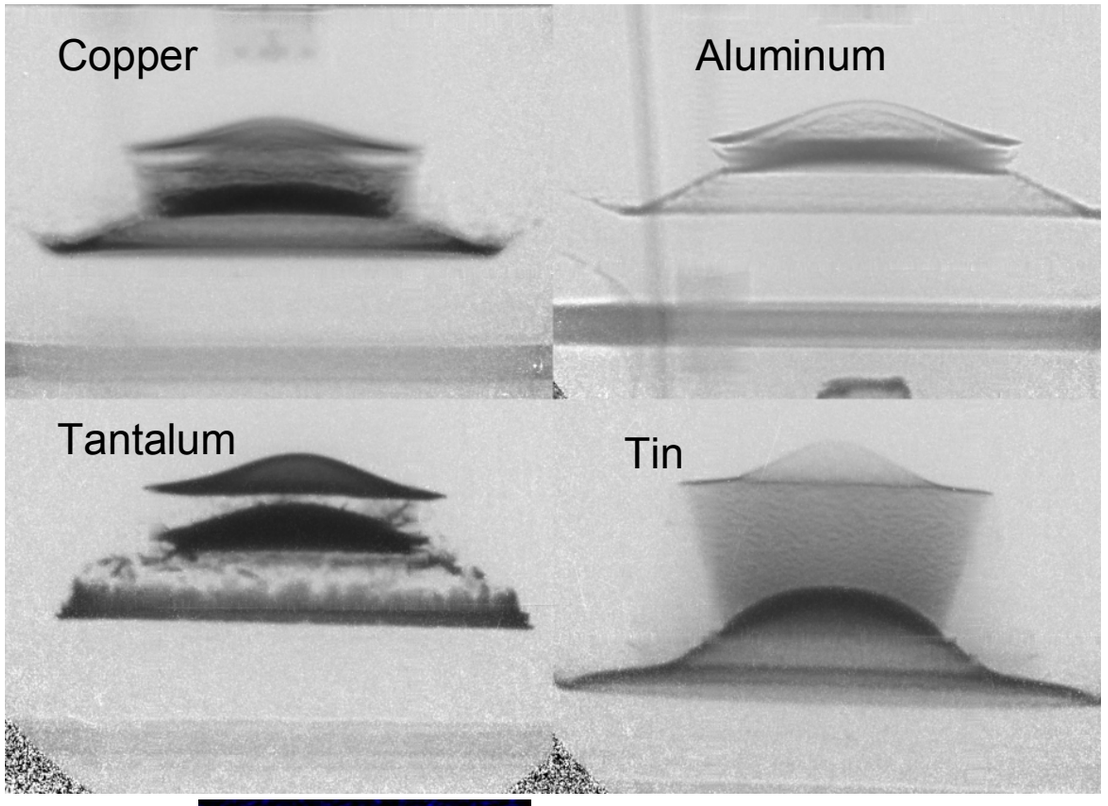

- Experiments were aimed at extending VISAR measurements below the leading spall layer.
- Proton radiographs reveal that the deepest damage layers are not well defined.
- Multiple pRad experiments show that damage formation deep within the metal is “statistical” in nature and dependent on metal.

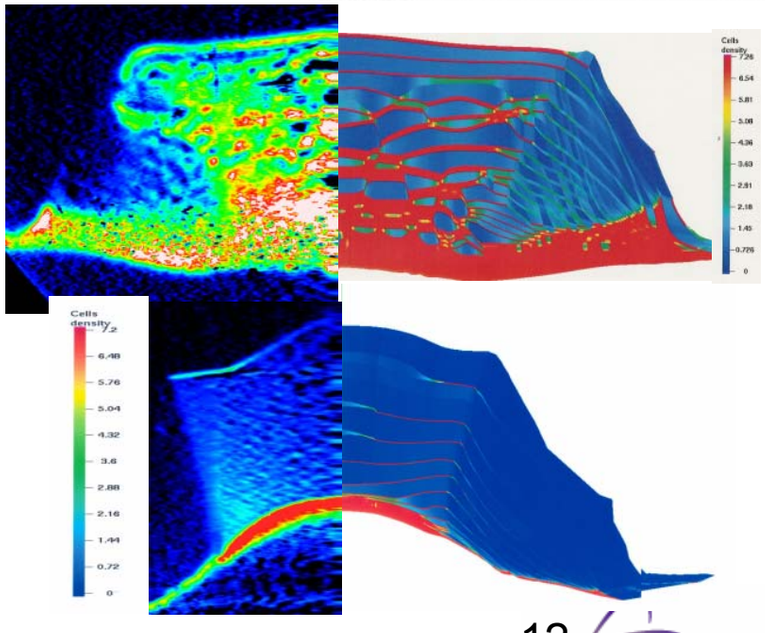

pRad has been used to study the failure of materials driven by point detonated high explosives

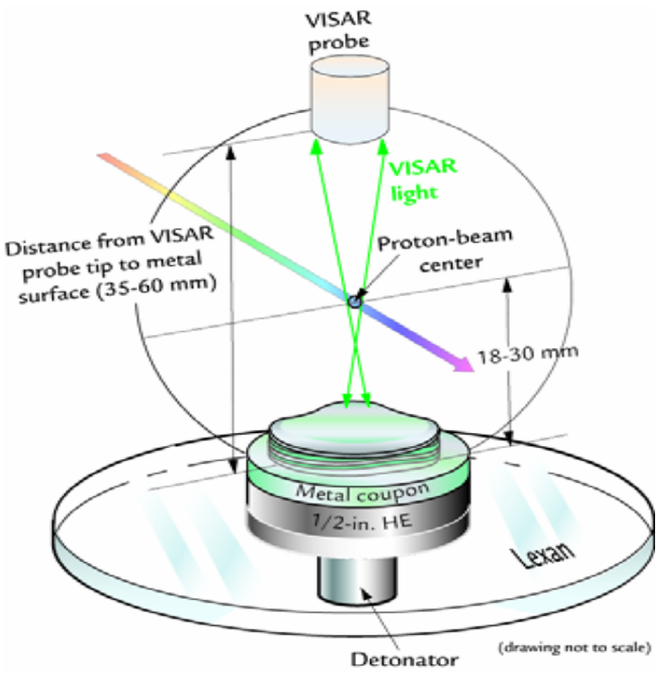

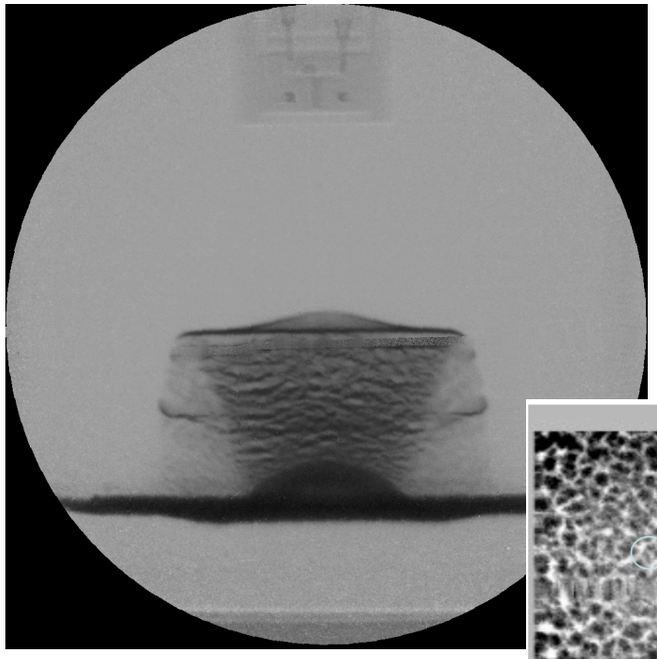

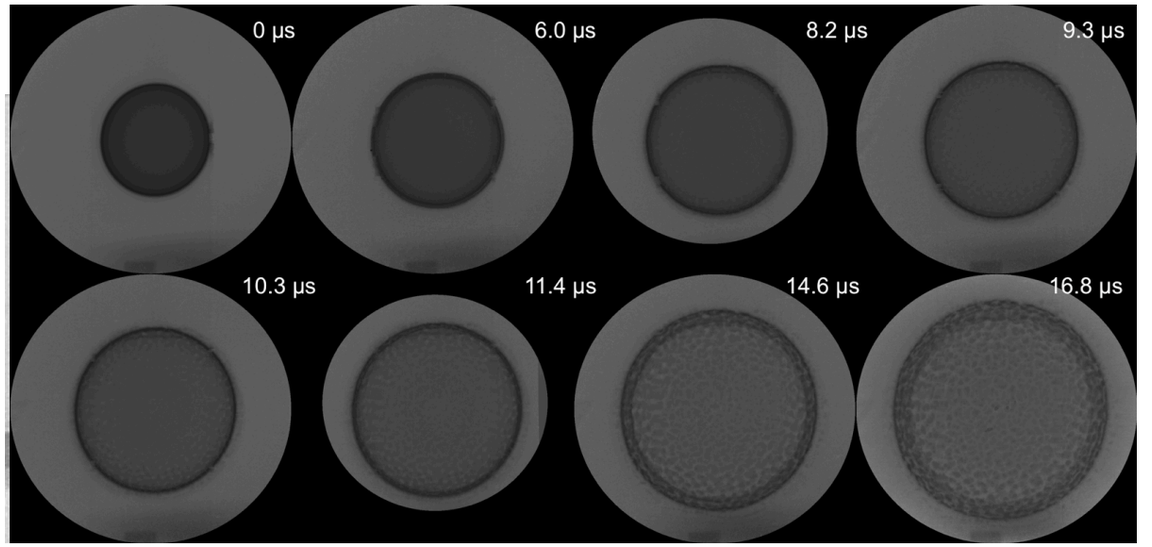

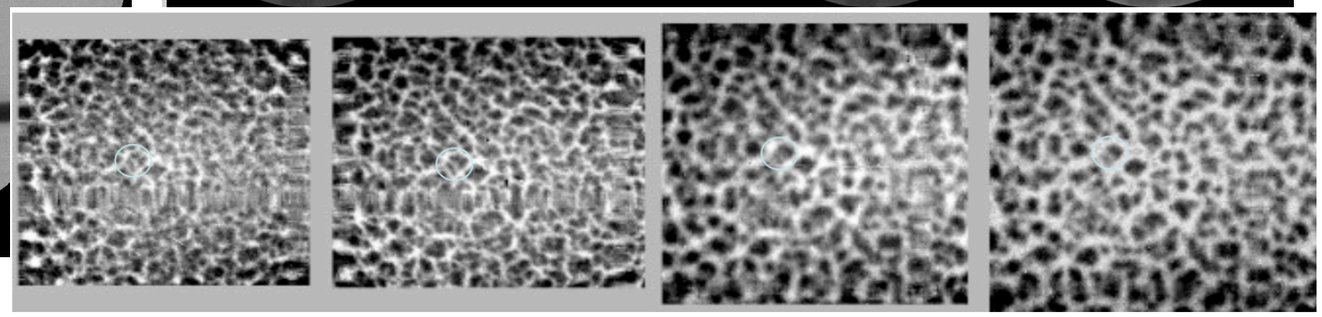

- Experiments were aimed at extending VISAR measurements below the leading spall layer.
- Proton radiographs reveal that the deepest damage layers are not well defined.
- Multiple pRad experiments show that damage formation deep within the metal is “statistical” in nature and dependent on metal.

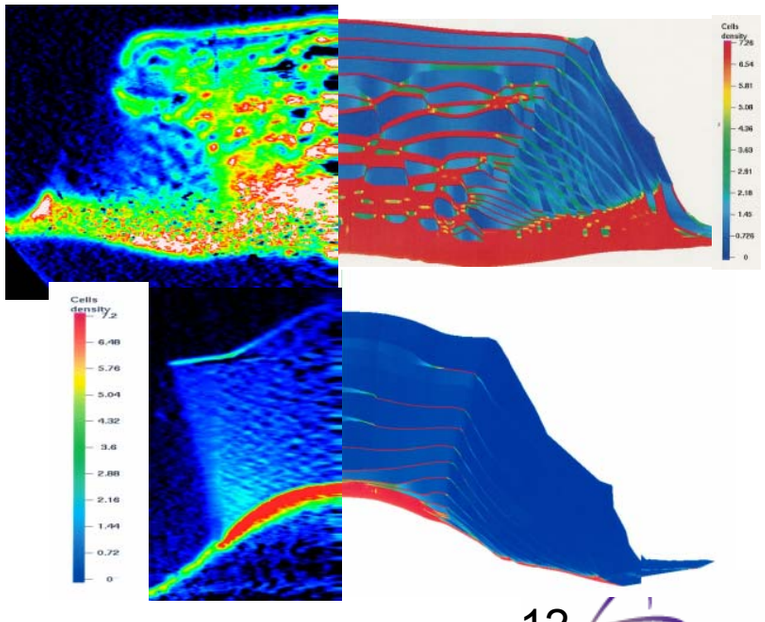

Material Strength Experiments

PTW fit to Hopkinson-Bar data*

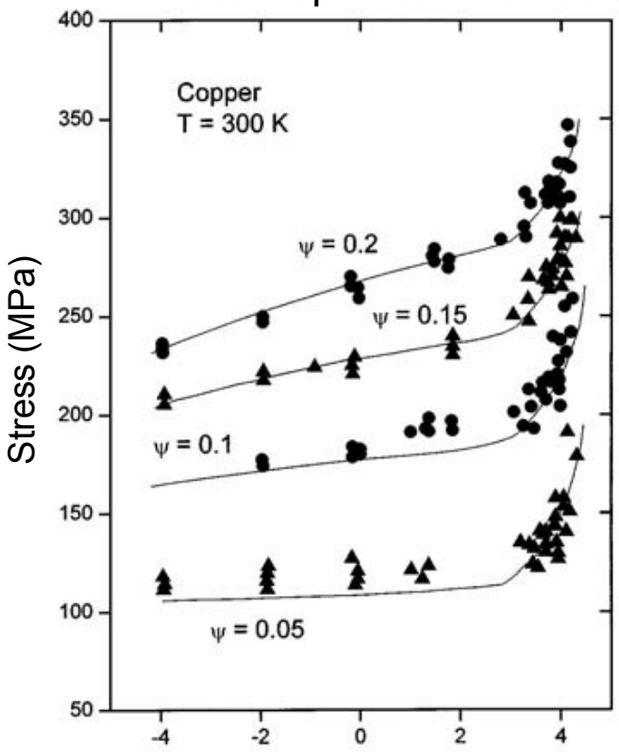

$Log_{10}[d\psi/dt]$ (s^{-1})

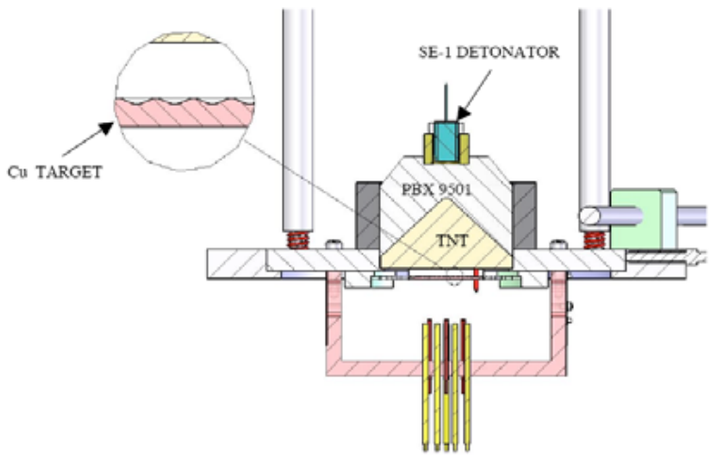

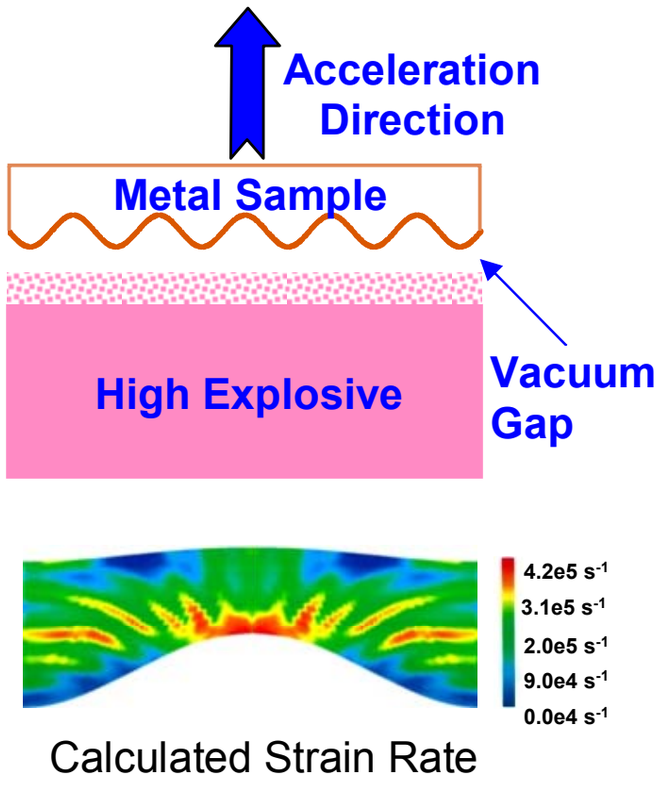

Calculated Strain Rate

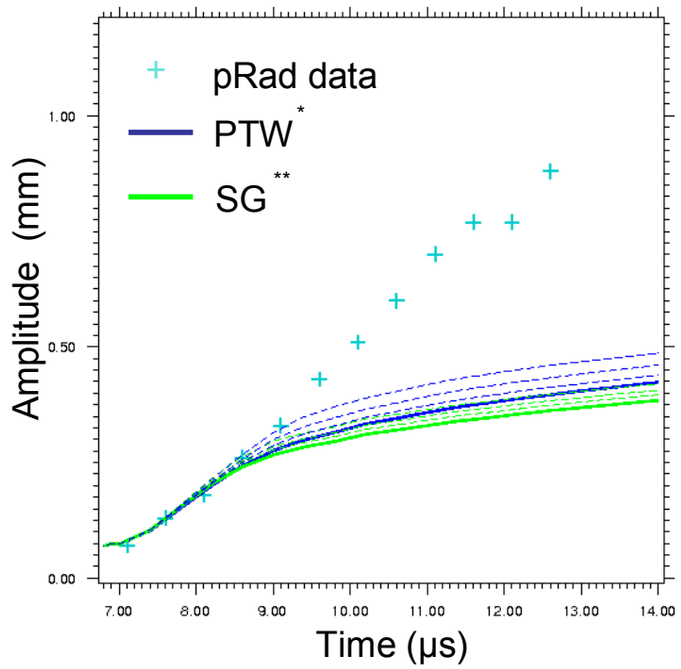

35 μm 55 μm

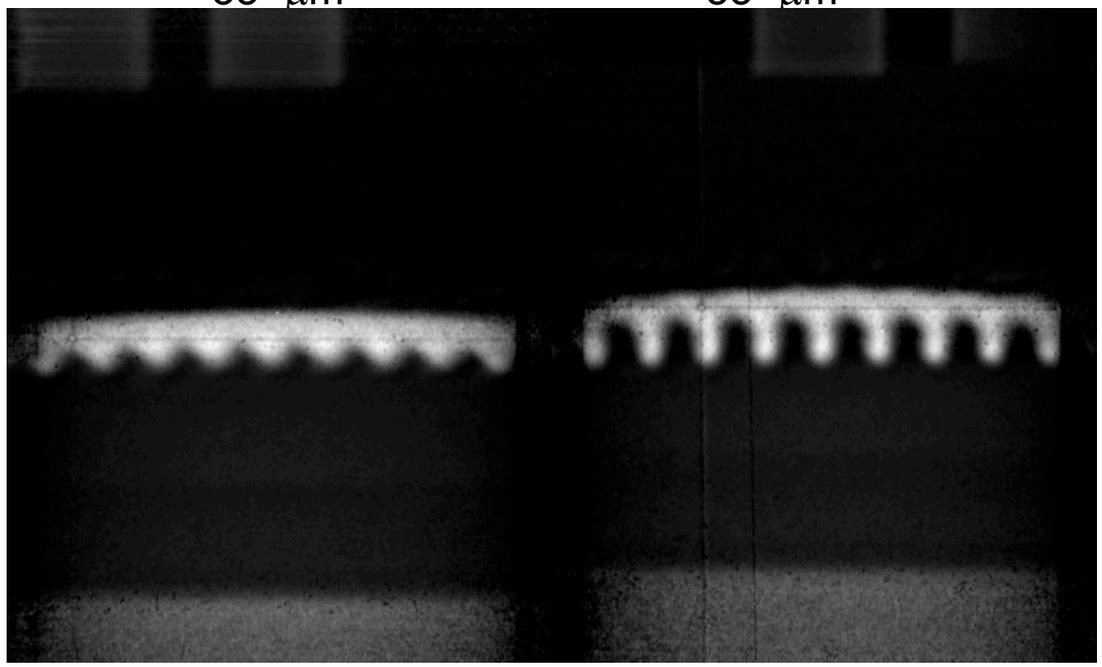

*D.L.Preston, et al. J.Appl. Phys. **93**, 211 (2003). ** D. J. Steinberg, et al. J.Appl. Phys. **61**, 1816 (1987).

Rictmyer-Meshkov Instability Growth in Gasses

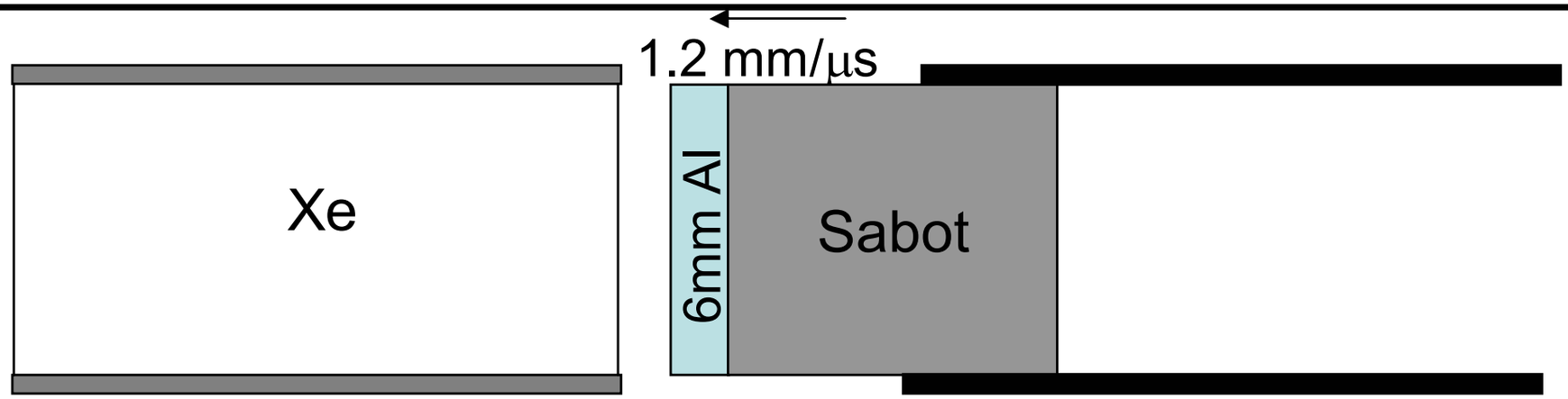

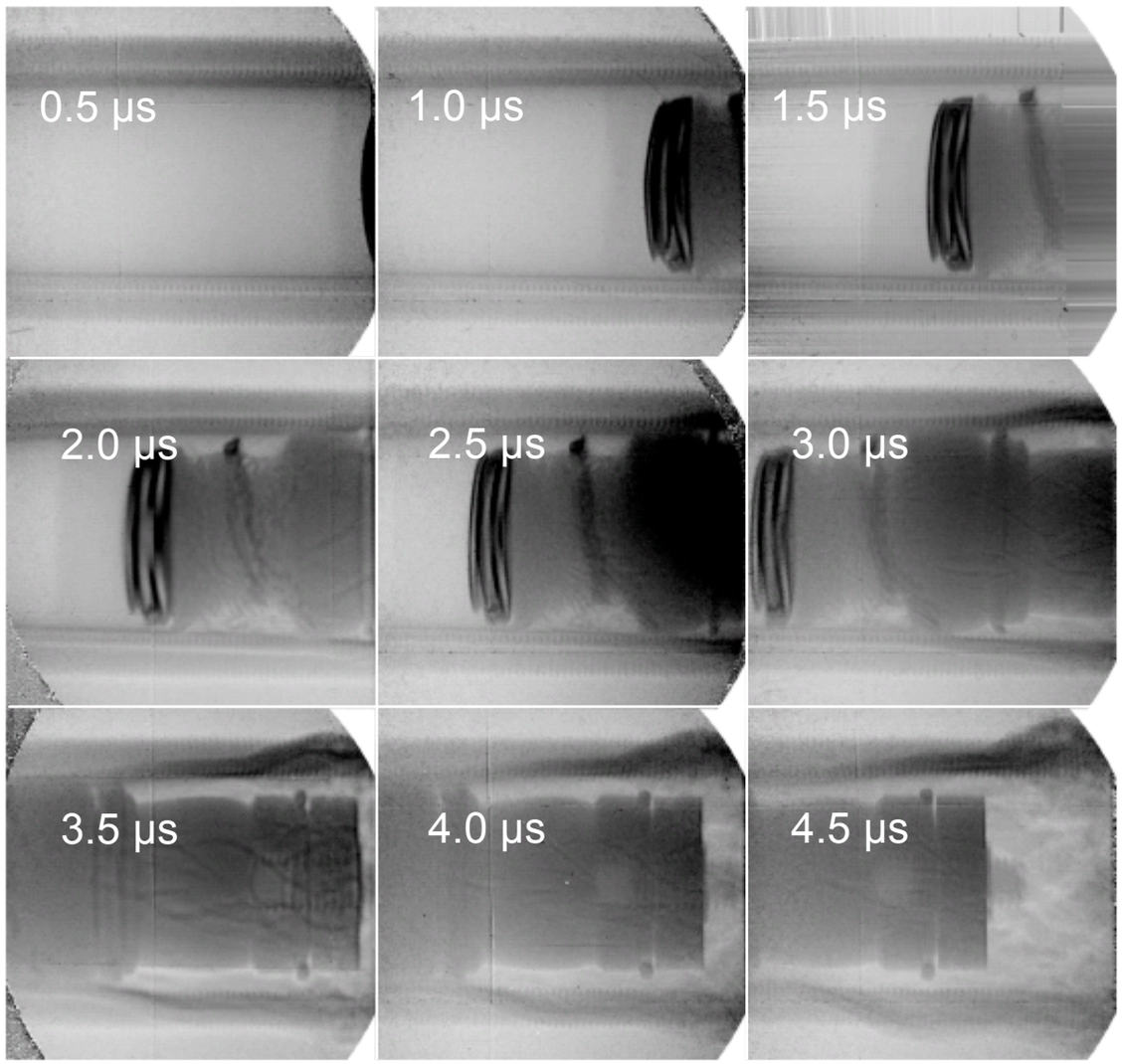

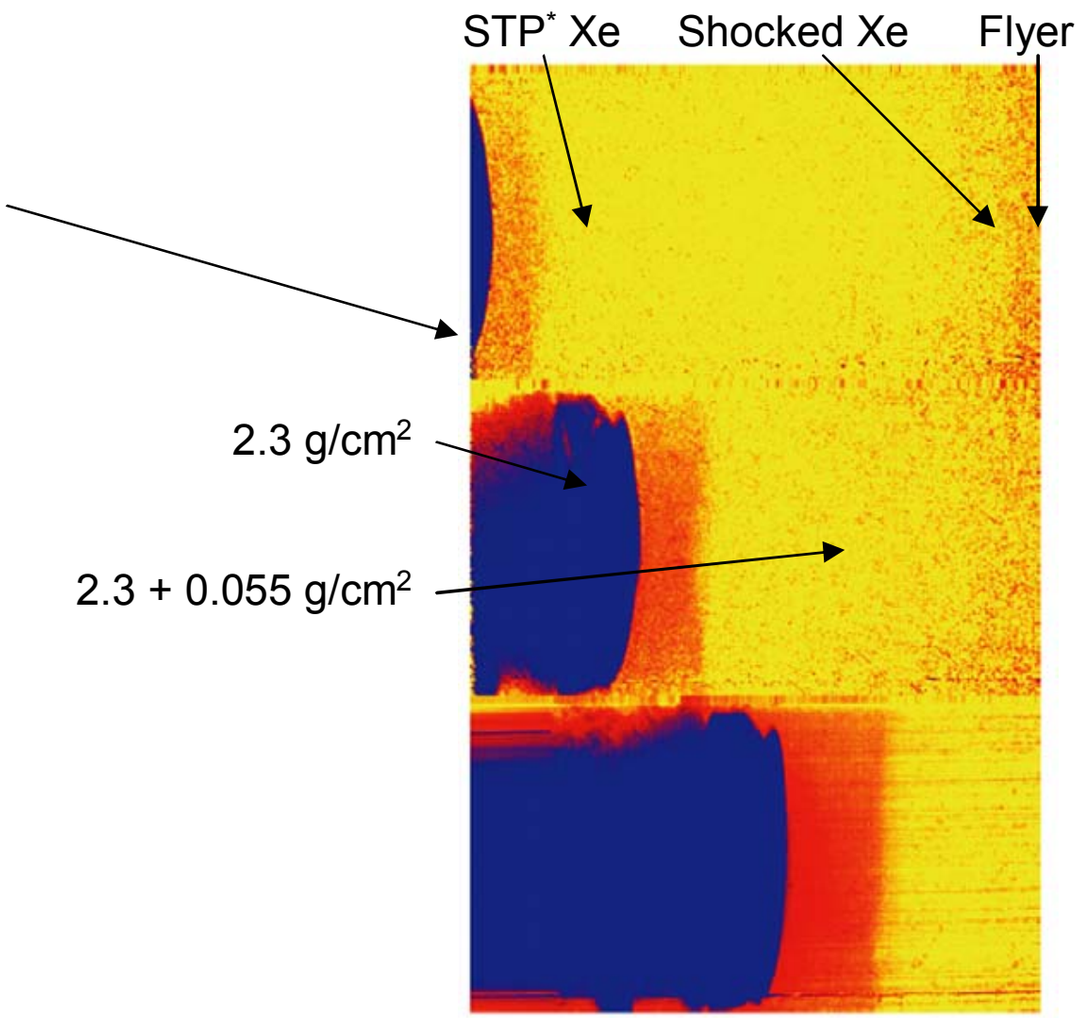

* Standard Temperature and pressure

Rictmyer-Meshkov Instability Growth in Gasses

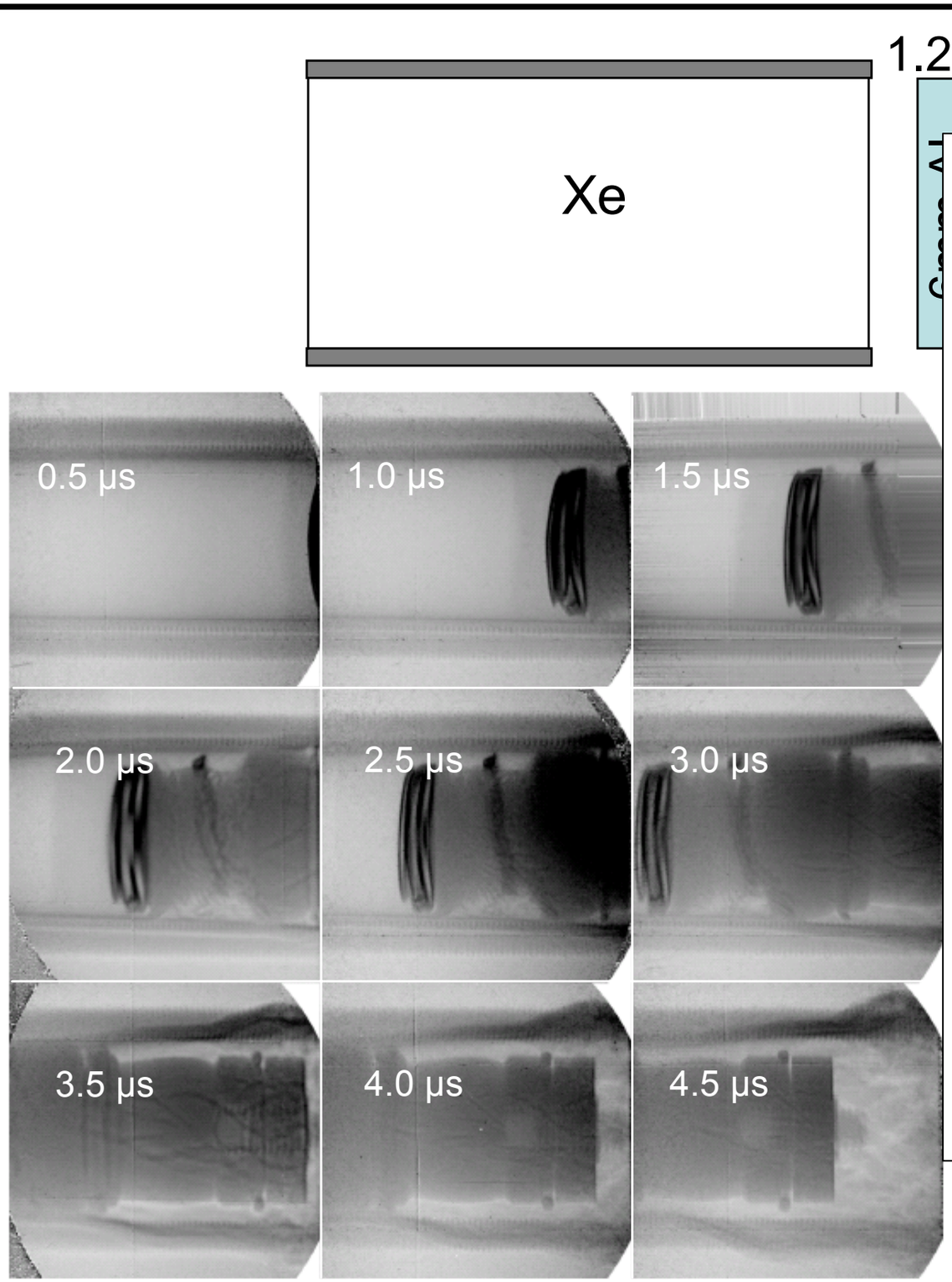

* Standard Temperature and pressure

Static Objects: Surrogate Nuclear Fuel Rods

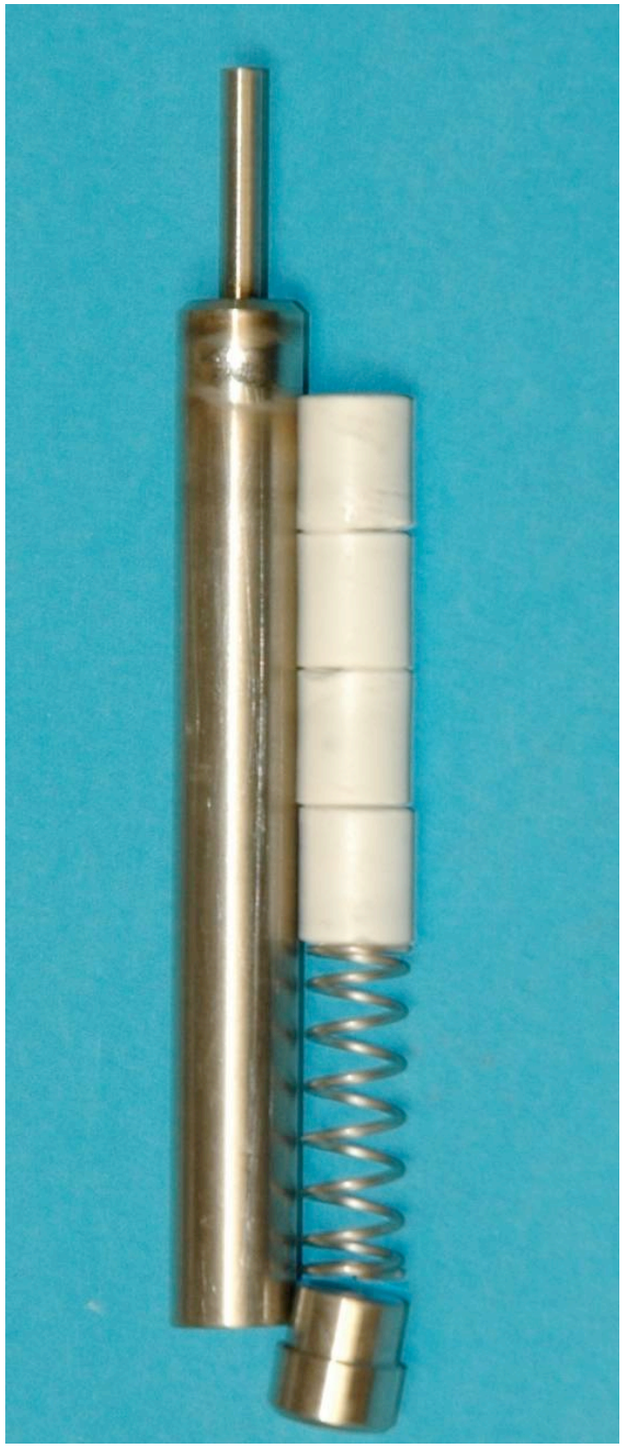

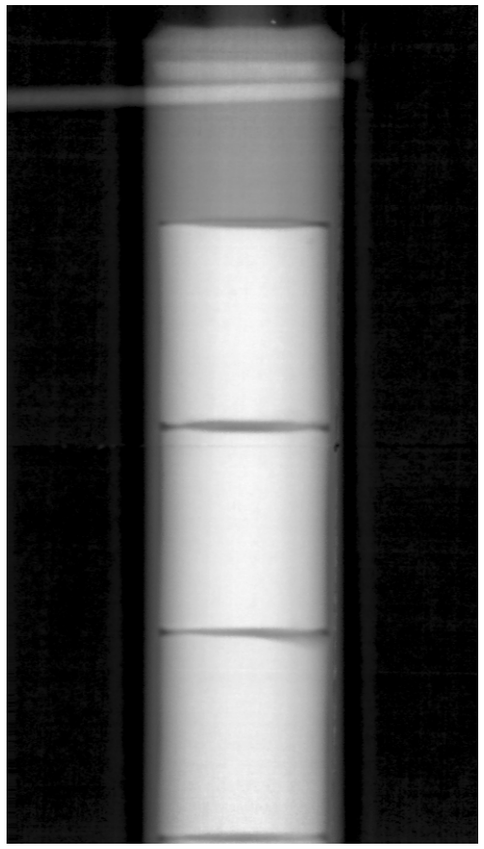

Halfnium Oxide surrogate fuel rod.

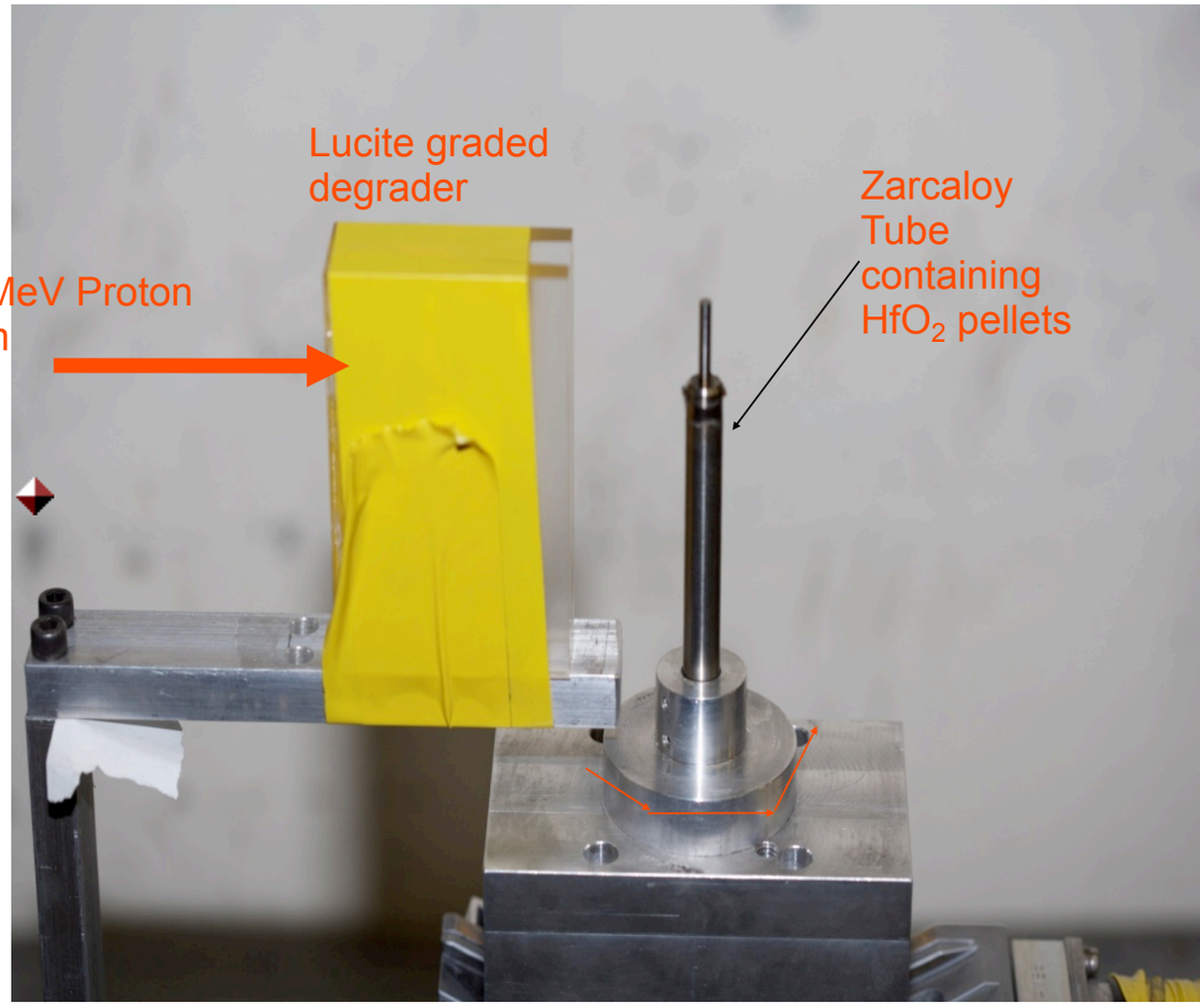

Filtered Back Projection

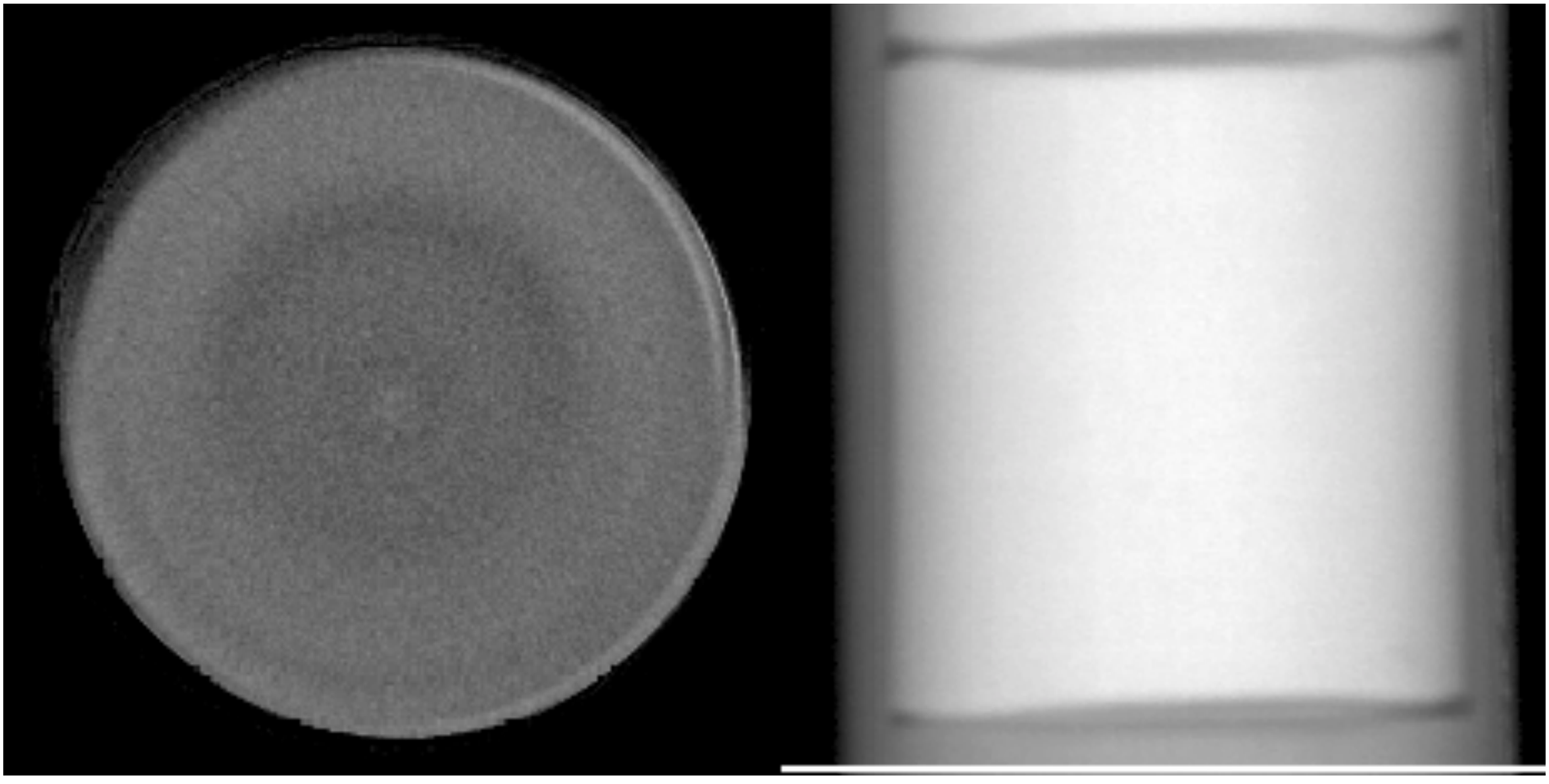

Filtered Back Projection:
Defects in Pellet #4, Slices 78 to 93

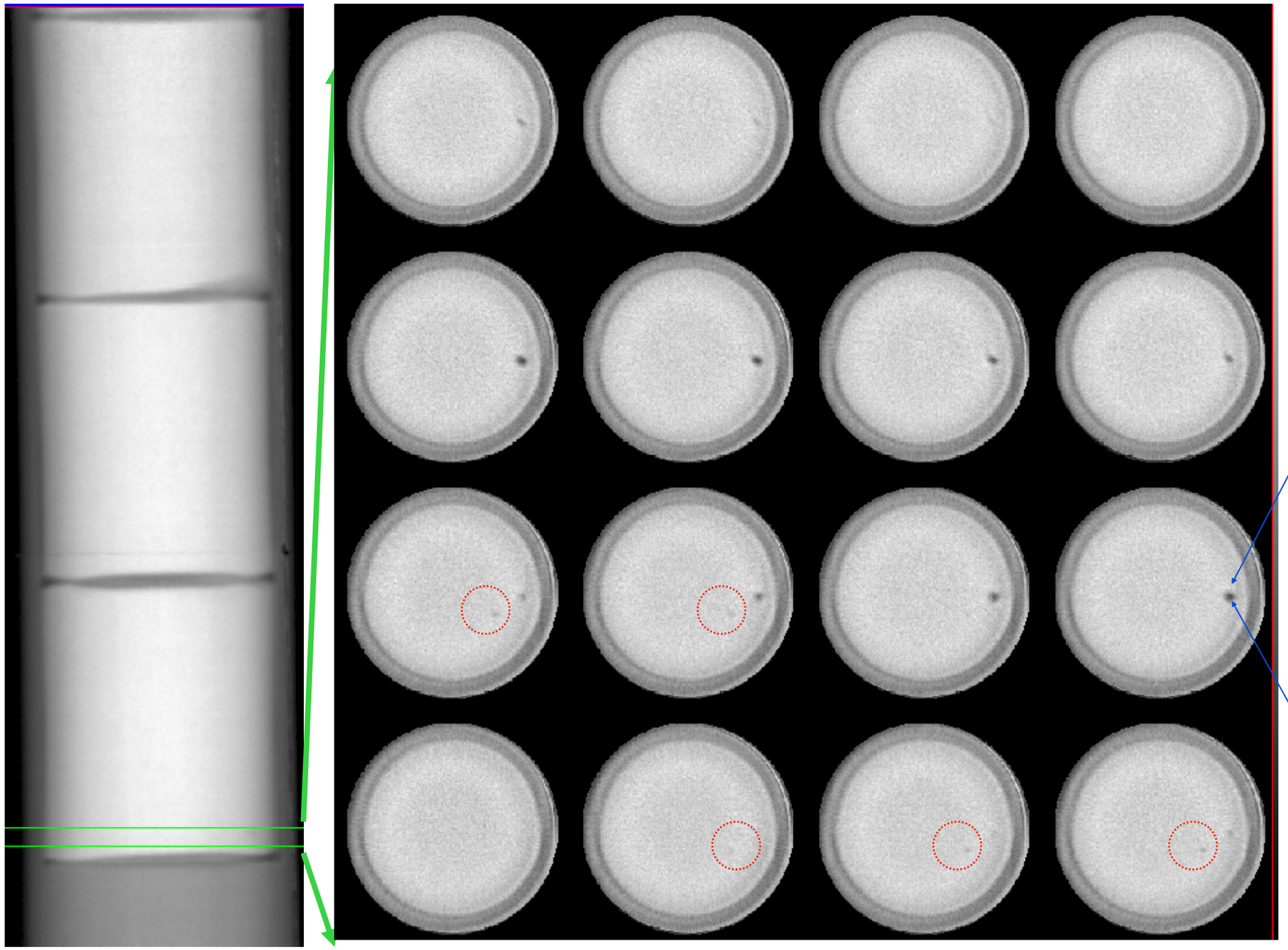

Resolution ~ 80 µm

$Diameter_{Inclusion}$ ~ 350 µm

$Length_{Inclusion}$ ~ 550 µm

Fainter 250 µm long by ~150 to 200 µm diameter inclusions are shown in the circles

Summary

<u>800 MeV Proton Radiography</u>

- Three imaging lens systems
  - 180 μm with 120 mm field of view
  - 65 μm with 42 mm field of view
  - 30 μm with 17 mm field of view
- 1-50 g/cm^2 object thickness.
- ~40 images, 100 ns exposure over < 1 ms

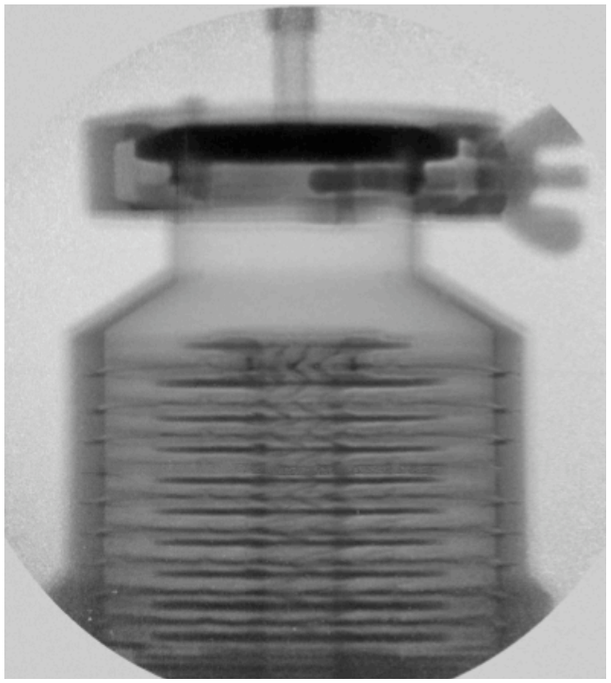

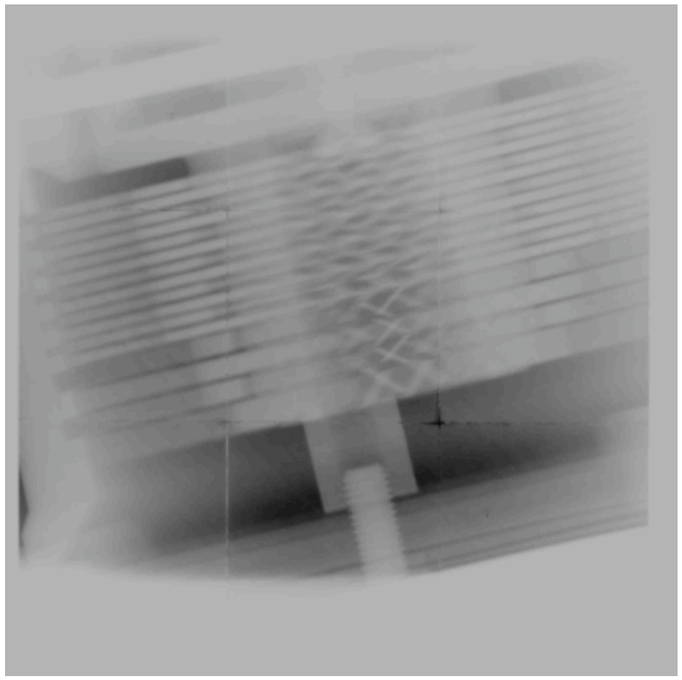

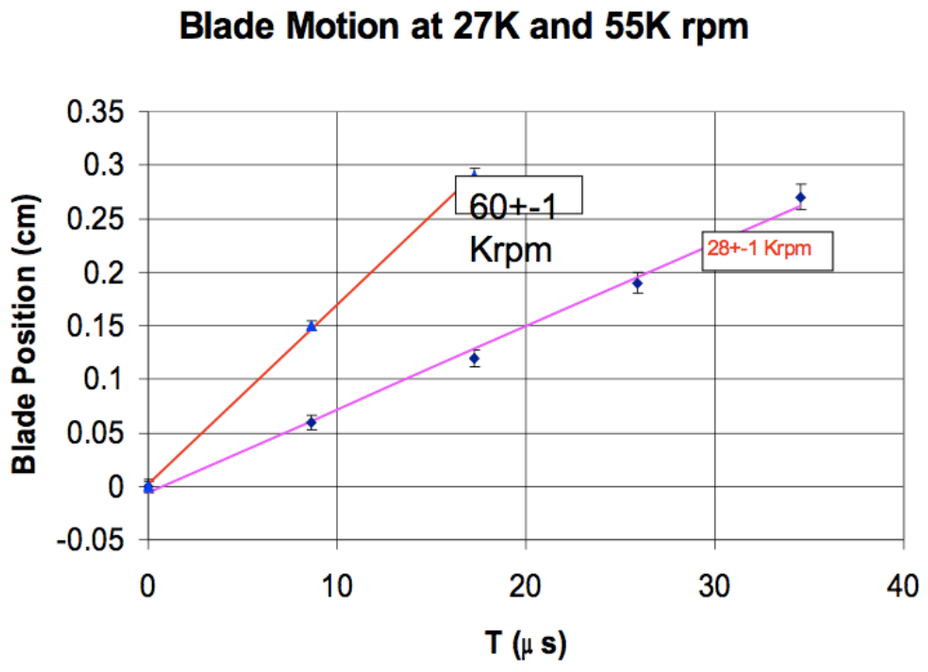

Turbo pump at 1.46 GeV/c and 7.5 GeV/c

Radiograph

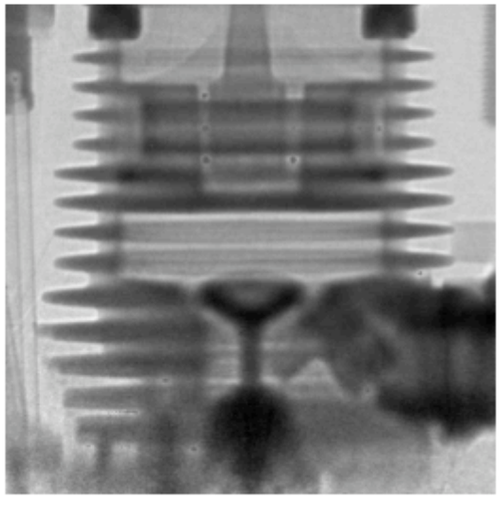

Areal density

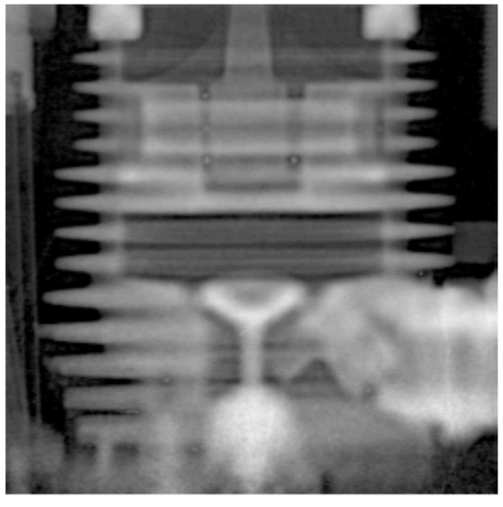

Volume density

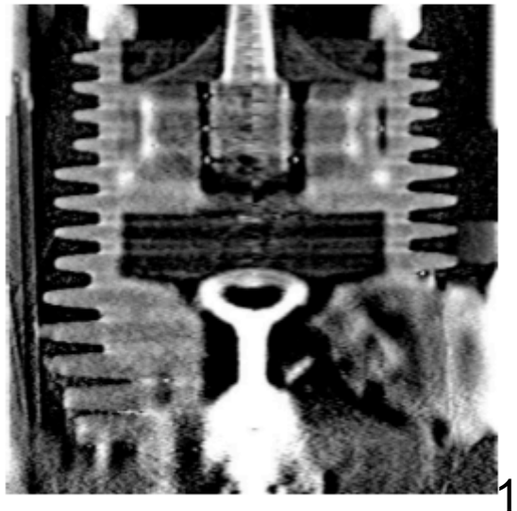

Sensitivity with 800 MeV Protons

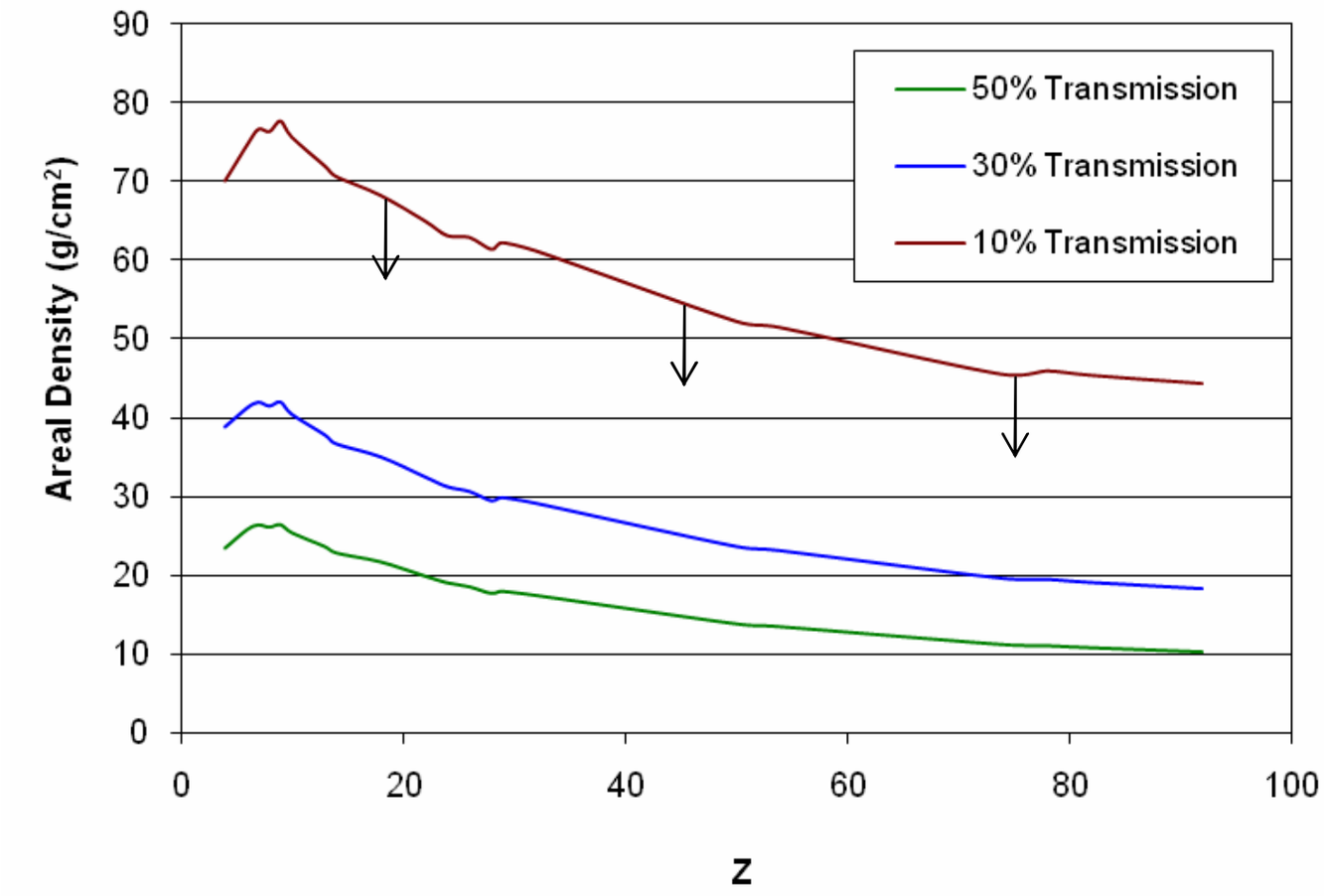

Areal density contours of constant transmission as a function of atomic number.

10% transmission is near the lower limit of reasonable transmission.

- Perform experiments less than ~50 g/cm^2 with 800 MeV proton Radiography

Dynamic Range of 800 MeV Proton Radigraphy

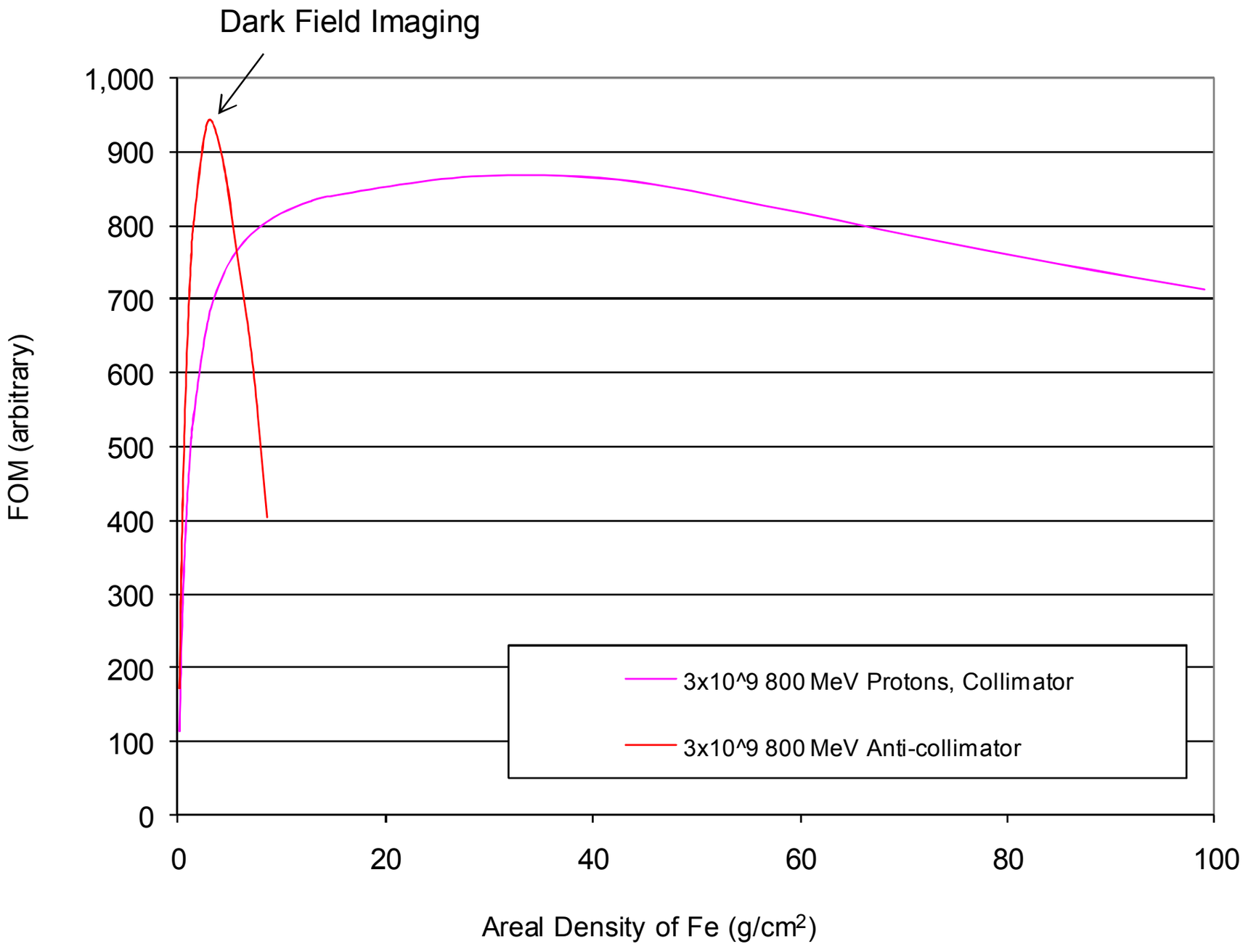

- 800 MeV proton radiography ranges from ~1 g/cm^2 up to 50 g/cm^2